

# The mosaic of horizontal cells in the macaque monkey retina: With a comment on biphaxiform ganglion cells

HEINZ WÄSSLE,<sup>1</sup> DENNIS M. DACEY,<sup>2</sup> TONI HAUN,<sup>2</sup> SILKE HAVERKAMP,<sup>1</sup>  
ULRIKE GRÜNERT,<sup>3</sup> AND BRIAN B. BOYCOTT<sup>4</sup>

<sup>1</sup>Max-Planck-Institut für Hirnforschung, Frankfurt, Germany

<sup>2</sup>Department of Biological Structure, University of Washington, Seattle

<sup>3</sup>Department of Physiology, University of Sydney, Sydney, Australia

<sup>4</sup>Institute of Ophthalmology, University College London, London, UK

(RECEIVED December 23, 1999; ACCEPTED February 23, 2000)

## Abstract

To further characterize the H1 and H2 horizontal cell populations in macaque monkey retinae, cells were injected with the tracer Neurobiotin following intracellular recordings. Tracer coupling between cells of the same type revealed all H1 or H2 cells in small patches around the injected cell. The mosaics of their cell bodies and the tiling of the retina with their dendrites were analyzed. Morphological differences between the H1 and H2 cells observable in Neurobiotin-labeled patches made it possible to recognize H1 and H2 cells in retinae immunolabeled for the calcium-binding proteins parvalbumin and calbindin, and thus to study their relative spatial densities across the retina. These data, together with the intracellularly stained patches, show that H1 cells outnumber H2 cells at all eccentricities. There is, however, a change in the relative proportions of H1 and H2 cells with eccentricity: close to the fovea the ratio of H1 to H2 cells is ~4 to 1, in midperipheral retina ~3 to 1, and in peripheral retina ~2 to 1. In both the Neurobiotin-stained and the immunostained retinae, about 3–5% of the H2 cells were obviously misplaced into the ganglion cell layer. Several features of the morphology of the misplaced H2 cells suggest that they represent the so-called “biphaxiform ganglion cells” previously described in Golgi studies of primate retina.

**Keywords:** H1 horizontal cells, H2 horizontal cells, Neurobiotin injection, Parvalbumin immunostaining, Calbindin immunostaining

## Introduction

Horizontal cells are retinal interneurons whose dendrites form the lateral elements in cone synaptic triads in the outer plexiform layer (OPL). In primates, horizontal cells are thought to contribute to the inhibitory receptive-field surround and to the color-opponent properties of bipolar cells and ganglion cells (Dacey, 1999). A clear picture of the number of distinct horizontal cell populations, their densities, and their cone connections is crucial for understanding the basis for the color-coding pathways. Two types of horizontal cells are well accepted: the H1 and H2 horizontal cells (Kolb et al., 1980; Boycott et al., 1987). The H1 cell has a large soma, stout, radiate dendrites, and a long axonal process with a terminal arbor connected to rods (Kolb, 1970; Boycott & Kolb, 1973; Kolb et al., 1980; Mariani, 1984; Boycott et al., 1987; Dacheux & Raviola, 1990). By contrast, the H2 cell has a smaller soma, finer, wavy dendrites, and an axon that contacts only cones (Kolb et al., 1980; Mariani, 1984; Gallego, 1985; Boycott et al., 1987). There is converging evidence that H2 cells contact all the long (L-), middle

(M-), and short (S-) wavelength-sensitive cones within their dendritic fields, with relatively more weight on the S-cone contacts, while H1 cells contact all L- and M-cones within their dendritic fields but make only sparse or no connections at all with S-cones (Ahnelt & Kolb, 1994*a,b*; Dacey et al., 1996; Goodchild et al., 1996; Chan & Grünert, 1998). A third type of horizontal cell—the H3 cell—has been reported in the human retina (Kolb, 1991; Kolb et al., 1992, 1994; Ahnelt & Kolb, 1994*a,b*). Though the H3 cell is notably similar to the H1 cell in dendritic and axonal morphology, its dendritic field is larger and often asymmetric, and some H3 cells have descending processes that terminate in the outer strata of the inner plexiform layer (IPL). Other investigators, however, have classified cells with these morphologies in the monkey retina as H1 cells because transitions between these two extreme forms can be seen at any given eccentricity, and processes descending and terminating in the IPL were not observed (Boycott & Kolb, 1973; Boycott et al., 1987; Boycott, 1988; Wässle et al., 1989*b*; Dacey et al., 1996; Goodchild et al., 1996; Chan et al., 1997; Chan & Grünert, 1998).

The mosaics of H1 and H2 cells of the monkey retina have previously been studied using immunocytochemical staining with antibodies against calcium-binding proteins and Golgi-impregnated retinae (Röhrenbeck et al., 1989; Wässle et al., 1989*b*). Both H1

Address correspondence and reprint requests to: Heinz Wässle, Max-Planck-Institut für Hirnforschung, Deutschordenstrasse 46, D-60528 Frankfurt/M., Germany. E-mail: Waessle@mpih-frankfurt.mpg.de

and H2 cells were found to be immunoreactive for parvalbumin, and their joint density across the retina could be measured. Antibodies against calbindin stained a single type of horizontal cell, but it was not clear which cell type was stained in these retinæ (Röhrenbeck et al., 1989; Martin & Grünert, 1992; Grünert et al., 1994). Therefore, the relative distributions of H1 and H2 cells were studied by determining the density of H1 cells in patches of Golgi-impregnated retinæ and then estimating the relative densities of H1 and H2 cells in the parvalbumin-stained retinæ (Wässle et al., 1989b). These results suggested that in central retina H1 cells outnumber H2 cells, while in peripheral retina the reverse is true.

In the present study, we reexamined the horizontal cell mosaics using intracellular injection of Neurobiotin following recordings from physiologically identified H1 and H2 cells (Dacey et al., 1996). Tracer coupling of homologous cell types (Vaney, 1991, 1993, 1994; Mills & Massey, 1994) revealed all H1 or H2 cells in small patches around the injected cell. We show that the cell bodies of H1 and H2 cells each form regular mosaics.

The tracer-coupled H1 and H2 cell mosaics made it possible to distinguish H1 and H2 cells immunolabeled for parvalbumin, while retinal sections double labeled for parvalbumin, calbindin, and Pep19 demonstrated that the calbindin-reactive horizontal cells are H2 cells. Using the Neurobiotin-stained peripheral patches of H1 and H2 cells and retinal sections double labeled for parvalbumin and calbindin, we determined the relative proportions of H1 and H2 cells across the retina. We now show that H1 cells outnumber H2 cells at all eccentricities. Finally, we observed H2 horizontal cells that were misplaced into the ganglion cell layer in both the tracer-coupled patches and the immunostained whole mounts. We suggest that these misplaced H2 cells represent the "biplexiform ganglion cells" described previously (Mariani, 1982; Zrenner et al., 1983).

## Methods

### *Neurobiotin labeling (Vaney, 1991)*

Eyes from macaque monkey (*Macaca nemestrina*, *Macaca fascicularis*, or *Macaca mulatta*) were obtained from the tissue program of the Washington Regional Primate Research Center. The retina, together with the pigment epithelium and choroid layer, was dissected and mounted in a superfusion chamber on the stage of a light microscope. Vital labeling of horizontal cell nuclei was achieved by incubating the eyecup before retinal dissection for ~20 min in Ames medium to which diaminophenylindole (DAPI) was added at a concentration of ~10  $\mu$ M. Intracellular recordings were made from horizontal cells penetrated under direct visual control (Dacey et al., 1996). At the termination of the recordings, cells were injected with Neurobiotin (Vector, Burlingame, CA). Retinæ were removed from the fixation chamber, fixed in phosphate-buffered (PB, 0.1 M; pH 7.4) 4% paraformaldehyde for ~2 h. The intracellular Neurobiotin was revealed, as described in detail by Dacey and Brace (1992), by a horseradish peroxidase (HRP) reaction product using the Vector ABC protocol (Vector, Elite kit). The diaminobenzidine (DAB) reaction product was intensified by a photochromic intensification, as described by Vaney (1992).

### *Immunocytochemical labeling of retinal whole mounts (Röhrenbeck et al., 1989)*

Four *Macaca fascicularis* monkeys were used in neurophysiological experiments before being killed by an overdose of Nembutal.

All experiments were performed according to the guidelines for the welfare of experimental animals issued by the Federal Government of Germany. The eyes were quickly enucleated, opened, and immersion fixed in phosphate-buffered paraformaldehyde as described above for 2 h. After dissection from the eyecup, the retinæ were washed in PB for 2 h, immersed in 30% sucrose in PB at 4°C overnight, quickly frozen in liquid nitrogen, and thawed. After three washes the tissue was treated with 0.1 M DL-lysine—10% normal goat serum (NGS)—0.5% Triton X-100 in PB for 4 h. Anti-cat parvalbumin sera (Stichel et al., 1986) and an anti rat calbindin monoclonal antibody (Röhrenbeck et al., 1989) were used at a dilution of 1:500 or 1:2000, respectively, in 3% NGS, 0.5% Triton X-100, and 0.05% sodium azide in PB. The retinæ were incubated in the primary antibodies for 3 days at 4°C. After a 4-h wash in PB, the retinæ were incubated with goat anti-rabbit, or goat anti-mouse secondary antibodies (Sigma, Deisenhofen, Germany, 1:80, medium as before) for 2 days at 4°C. For visualization the peroxidase-antiperoxidase (PAP) method was used (Sternberger & Sternberger, 1986). After rinsing in PB, the retinæ were treated with rabbit-PAP, or mouse-PAP (Sigma, Deisenhofen, Germany, 1:150, medium as before, but without sodium azide) for 2 days at 4°C. Following three washes in PB, retinæ were incubated in 0.05% 3,3'-diaminobenzidine (DAB; Sigma, Deisenhofen, Germany) in PB for 10 min, then for an additional 20 min in 0.05% DAB to which hydrogen peroxide was added to a final concentration of 0.01%. Retinæ were fixed onto gelatinized glass slides (Wässle et al., 1975) ganglion cell side up, dehydrated in ethanol, cleared in xylene, and mounted with Permount (Fisher, Pittsburgh, PA).

### *Immunocytochemical labeling of horizontal sections (Grünert et al., 1994)*

Four retinæ of juvenile macaque monkeys (*M. fascicularis*) were obtained after unrelated physiological experiments. Animals were perfusion fixed under deep Nembutal anesthesia with phosphate-buffered 4% paraformaldehyde and 0.1% glutaraldehyde. After perfusion and dissection, retinæ were immersion fixed in 4% paraformaldehyde for 2–6 h then rinsed in PB containing 0.01% sodium azide for several days. Retinæ were immersed in 30% sucrose in PB overnight before sectioning. Horizontal frozen sections 70  $\mu$ m thick were taken with a sliding microtome and processed free floating, as described above for retinal whole mounts. A rabbit polyclonal antibody against rat calbindin (CaBP D-28K; provided by Dr. C.W. Heizmann, Zürich; Pinol et al., 1990) was used at a dilution of 1:4000 or 1:8000. Immunoreactivity was demonstrated by the avidin-biotin peroxidase complex (ABC) method. Goat anti-rabbit biotin (Sigma; B-8895) and Extravidin-Peroxidase (Sigma; E-2886) were used.

### *Double-immunocytochemical labeling of vertical sections*

Three retinæ of *M. fascicularis* were obtained after unrelated physiological experiments. Animals were deeply anesthetized and killed by an overdose of Nembutal. One retina was immersion fixed in 2% paraformaldehyde for 30 min. One retina was obtained after perfusing the animal for 10 min with 4% paraformaldehyde without additional fixation by immersion. One retina was obtained after perfusing the animal with 4% paraformaldehyde followed by an additional fixation by immersion in 4% paraformaldehyde for several hours. Vertical sections 12  $\mu$ m thick were taken on a cryostat and collected onto gelatinized slides. For double immuno-

fluorescence, they were incubated in a mixture of one of the monoclonal antibodies and one of the polyclonal antisera (parvalbumin: rabbit anti-rat parvalbumin, Swant, dilution 1:1000; calbindin: mouse anti-rat calbindin, clone CL-300, Sigma, dilution 1:1000; Pep19: rabbit anti Pep19, kind gift of J.I. Morgan, Memphis, TN, Ziai et al., 1986, dilution 1:2000; parvalbumin: mouse anti-rat parvalbumin, Sigma, dilution 1:10000). After washing in PB, secondary antibodies were applied for 1 h. These included goat anti-mouse IgG or anti-rabbit IgG conjugated to either Alexa TM 594 (red fluorescence) or Alexa TM 488 (green fluorescence: Molecular Probes, Eugene, OR) all diluted 1:500.

### Light microscopy

Maps of the whole mounts were drawn at a final magnification of 25 $\times$  and blood vessels and other landmarks (blind spot, fovea) were inserted together with the Neurobiotin-injected patches. The maps were used to precisely measure the eccentricity and retinal position of the patches. For mosaic measurements, fields containing labeled horizontal cells were drawn at a final magnification of 400 $\times$  or 1000 $\times$ . All measurements (nearest-neighbor distances) were taken from these drawings.

For light-microscopic analysis of double-labeled sections appropriate fluorescence filters were used (Alexa 488: 450–490, FT 510, LP 520; Alexa 594: BP 546, FT 580, LP 590). In some instances, very strong red fluorescence was also visible with the green filter. This was blocked by an additional green fluorescence filter (515–565) inserted into the microscope tube. Fluorescence photomicrographs were taken on Kodak TMY 400 film (Eastman-Kodak, Rochester, NY). All other photomicrographs were taken with Nomarski optics (differential interference contrast) on a Zeiss Axiophot microscope using AGFA professional, 25 ASA, black-and-white film (AGFA-Gevaert, Leverkusen, Germany).

## Results

Patches of H1 and H2 horizontal cells in monkey retinae were revealed by intracellular injection of Neurobiotin following physiological recordings (Figs. 1A and 2A). Some of the patches comprised several hundred, others only a few, cells. Close to the injection sites cells were intensely labeled, while towards the periphery of the patch the label gradually faded away. Dendrites and axons were visible in well-stained patches (Figs. 1B and 2B), making it possible to discriminate H1 and H2 horizontal cells. The dendrites bore aggregates of terminals contacting the cone pedicles. Altogether 11 patches were analyzed in detail: one from midperipheral retina (5.8-mm eccentricity), the others from peripheral, temporal retina (8.5–12 mm eccentricity). In peripheral retina, H1 cells have polygonal, large cell bodies and stout, long dendrites which form a dense network of processes (Fig. 1B). H2 cells have smaller cell bodies and their dendrites are more delicate and more curved (Fig. 2B). In most of the patches the distribution of cones could be studied by changing the focal plane (not illustrated), and it was possible to estimate the cone densities and the cone to horizontal cell ratios (Table 1).

### The mosaic of H2 horizontal cells

The H2 cell patch of Fig. 2A was analyzed in more detail in Fig. 3. The mosaic of cell bodies was drawn directly from the microscope with the aid of a drawing apparatus (Fig. 3A). The cell bodies

appear to be regularly spaced, and close neighbors occur only rarely.

We measured the distance from each single cell to the nearest neighbor: the resulting distribution (Fig. 3B) has a Gaussian shape with a mean distance of 29.3  $\mu\text{m}$  and a standard deviation of 6.8  $\mu\text{m}$ . The ratio of the mean distance to the standard deviation provides a convenient test for the regularity of such retinal cell mosaics (Wässle & Riemann, 1978). In the case of Fig. 3B, a regularity index of 4.3 was found. H2 horizontal cells in this patch of the monkey retina appear to be as regularly distributed as A-type horizontal cells of the cat, for which a nearest-neighbor regularity index of 4.7 has been calculated (Wässle & Riemann, 1978).

We also studied the number of cones contacted by individual H2 horizontal cells from the terminal aggregates formed by the dendritic tips. Four cells from the center of the patch in Fig. 2B were analyzed and found to contact 15, 17, 15, and 16 cones (mean  $15.75 \pm 0.95$ ), respectively. The cone density in the patch of Figs. 2A and 3A was 3229 per  $\text{mm}^2$  and the H2 cell density was 562 per  $\text{mm}^2$ . From these data we can calculate the number of H2 cells that an individual cone feeds into. This so-called divergence of the cone signal (Freed et al., 1987) is calculated by multiplying the H2 cell density (562) by the mean number of cones contacted (15.75) and dividing it by the cone density (3229). The result of the calculation is 2.74, indicating that each individual cone in the peripheral monkey retina contacts between 2 and 3 H2 horizontal cells.

The dendrites of neighboring H2 horizontal cells showed considerable overlap (Fig. 2B), and it was often difficult to delineate the dendritic fields of individual H2 cells within this network. A measure of this overlap is the coverage factor, calculated by multiplying the density of the cells with the average dendritic field area. The patch of H2 cells shown in Figs. 2A and 3A had a coverage factor of 2.2. The anatomical constraints of this coverage are illustrated in Fig. 3C, where the dendritic tree of the H2 cell in the center has been drawn and the surrounding H2 cell bodies have been inserted. The dendritic tree is smaller than the area defined by the neighboring cell bodies, suggesting that these neighbors provide a “stop signal” for the growth of H2 cell dendrites during retinal development.

### The mosaic of H1 horizontal cells

A drawing of the H1 cell patch of Fig. 1A is shown in Fig. 4A. The total diameter of this patch was approximately 1 mm, containing more than 800 tracer-coupled H1 cells; only the central portion of 364 labeled H1 cells is shown in Fig. 4A. The cell bodies appear to be regularly spaced. Inspection of Fig. 1B, however, demonstrates that it is impossible to delineate the dendritic trees of individual H1 cells: the network of their processes is too dense, suggesting there is considerable overlap. We measured the distances between nearest neighbors (Fig. 4B): the resulting histogram has a Gaussian shape with a mean distance of 24.4  $\mu\text{m}$  and a standard deviation of 6.0  $\mu\text{m}$ . The regularity index was 4.1, indicating that monkey H1 and H2 horizontal cells as well as cat A- and B-type horizontal cells form mosaics of comparable precision. Since it was not possible to delineate individual dendritic trees from the network, we could not assess their cone contacts directly. However, we know from Golgi-stained retinae (Boycott & Kolb, 1973; Wässle et al., 1989b) and from DiI-labeled retinae (Goodchild et al., 1996) that peripheral H1 cells contact between 20 and 45 cone pedicles. The H1 cell density in the patch of Fig. 4A was 890 cells per  $\text{mm}^2$  and the cone density was 2973 per  $\text{mm}^2$ . Assuming an individual H1 cell contacts an average of

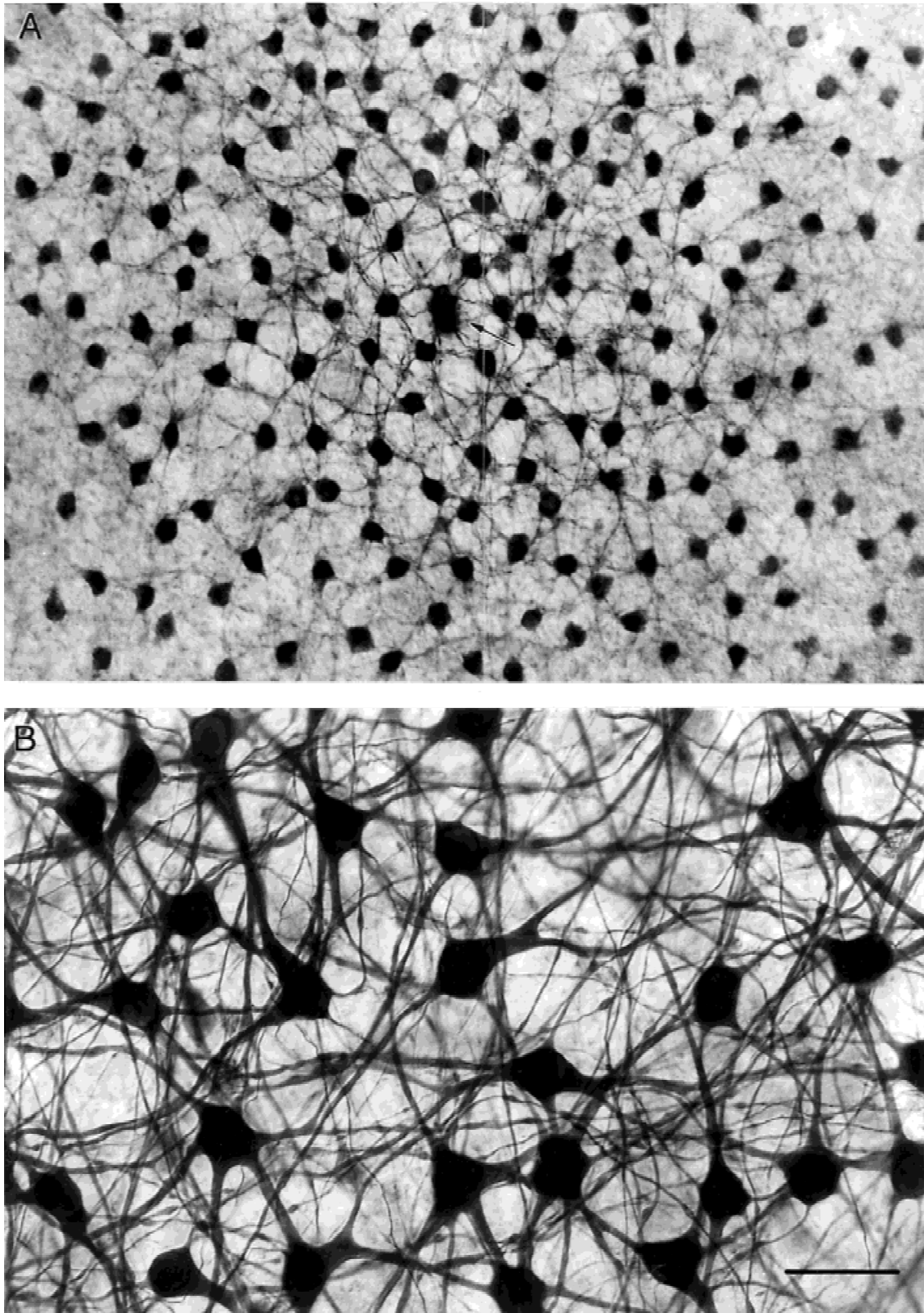


**Fig. 1.** The mosaic of tracer-coupled H1 horizontal cells following intracellular injection of Neurobiotin. (A) Nomarski micrograph of a whole mount of peripheral monkey retina. The H1 horizontal cell in the center (arrow) was injected with Neurobiotin and H1 cells in a patch of approximately 500- $\mu\text{m}$  diameter were stained through tracer coupling. The intensity of staining gradually decreased towards the periphery of the patch. (B) High-power micrograph of another H1 cell patch showing the dense network of H1 cell processes. Scale bar = 50  $\mu\text{m}$  in A and 25  $\mu\text{m}$  in B. Eccentricity = 8.6 mm in A and 12 mm in B.

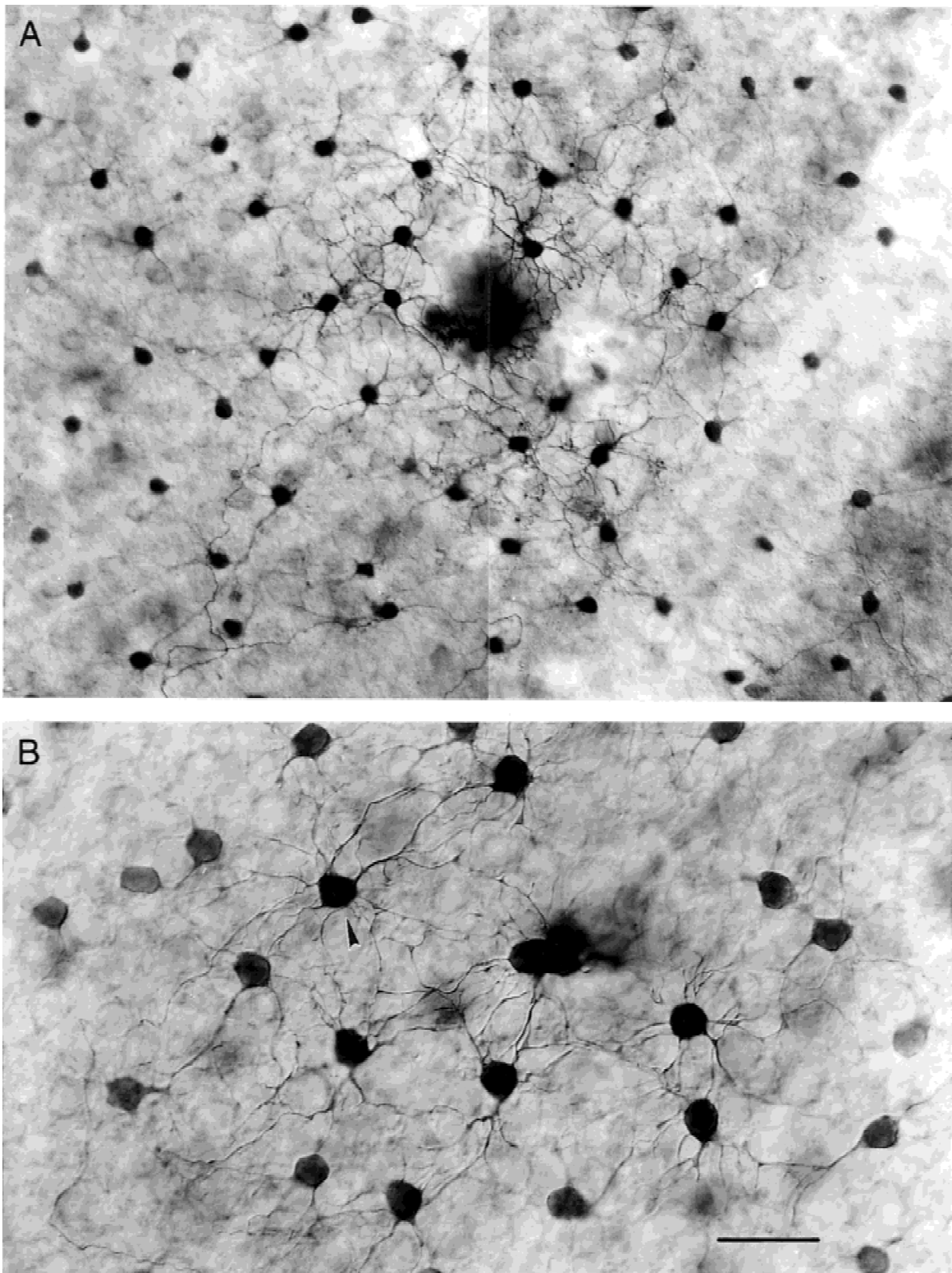


**Fig. 2.** The mosaic of tracer-coupled H2 horizontal cells following intracellular injection of Neurobiotin. (A) Low-power Nomarski micrograph of a whole mount of peripheral monkey retina. The dark spot in the center obscures the H2 horizontal cell that was injected. More than 200 H2 cells were stained through tracer coupling. The broad diagonal band in the right part represents a blood vessel. Dendrites and axons of the cells in the center of the patch are well stained. (B) High-power micrograph of another H2 cell patch. The delicate, wavy dendrites of the H2 cells become apparent. A drawing of the cell indicated by the arrowhead is presented in Fig. 3C. The cell with the black halo in the center was injected with Neurobiotin. Scale bar = 43  $\mu\text{m}$  in A and 25  $\mu\text{m}$  in B. Eccentricity = 9.75 mm in A and 8.5 mm in B.

**Table 1.** The density of horizontal cells and cones measured in neurobiotin injected and tracer coupled patches of monkey retinae

Patch (animal)	Eccentricity (mm)	H-cell density (1/mm <sup>2</sup> )	Cone density (1/mm <sup>2</sup> )	Cones/H-cell
1 (91144)	10.4	H2: 417	3278	7.9/1
2 (J91371)	9.8	H2: 656	3868	5.9/1
3 (T84102)	12.0	H2: 721	4669	6.5/1
4 (L91139)	11.2	H2: 541	3824	7.1/1
5 (F82383)	8.5	H2: 787	4950	6.3/1
6 (81274)	9.8	H2: 561	3229	5.8/1
7 (J87155)	11.5	H1:1183	3900	3.4/1
8 (F82402)	10.4	H1:1336	3991	3/1
9 (T79476)	10.9	H1: 818	3200	3.9/1
10 (F89280)	5.8	H1:3333	6763	2/1
11 (89211)	11.7	H1: 890	2973	3.3/1

30 cone pedicles, we calculated the divergence of the cone signal as 9 ( $890 \times 30/2973$ ). This means that, on average, a cone pedicle of peripheral monkey retina makes synaptic contacts with 9 individual H1 horizontal cells. This is the consequence of the substantial overlap within the H1 cell network (Fig. 1B).

In one patch of Neurobiotin-labeled H1 cells, the dendritic tree of the injected cell appeared well filled, while the network of coupled H1 cells appeared only lightly labeled. Fig. 4C is a drawing of this patch. It is obvious, that the dendritic tree of the injected H1 cell is much wider than the distance to the next neighbors. As discussed in detail by Wässle et al. (1989b), it makes no sense to fit a circular outline around the dendritic tree of such a cell and to calculate from this area a coverage factor, because these cells make cone contacts only along their major dendrites and not in between (Chan et al., 1997). It has to be emphasized, and it has been shown before, that H1 cells in the central retina of the monkey have circular, compact dendritic fields, that are comparable to H2 cells (Fig. 3C), delineated by the cell bodies of the surrounding neighbors (see Fig. 13 of Wässle et al., 1989b). In peripheral retina there appears to be a growth of the dendrites of H1 cells far beyond their next neighbors (Fig. 4C).

#### The combined mosaic of H1 and H2 horizontal cells

In several Neurobiotin-labeled patches both H1 and H2 cells appeared to be labeled (Fig. 5). Whether this is the result of heterologous tracer coupling between H1 and H2 cells (Vaney, 1994), or whether two cells were impaled with the electrode, has to be left open at present because there was leakage of Neurobiotin around the injection sites. In such patches usually one of the two cell types appeared to be more prominently labeled. In Fig. 5, the dendritic

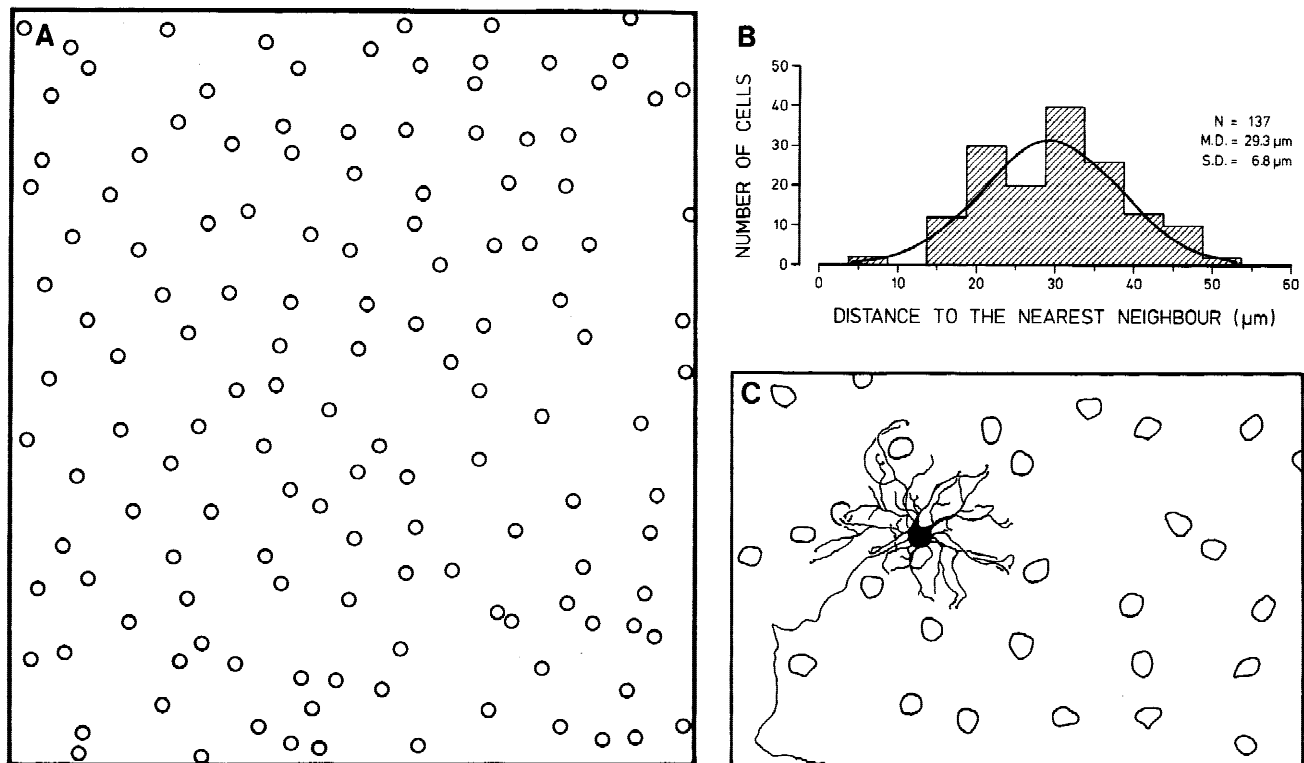


**Fig. 3.** (A) Drawing of the H2 horizontal cells taken from the patch in Fig. 2A. The cell bodies appear regularly spaced and immediate neighbors (twins) appear rarely. (B) Nearest-neighbor histogram calculated for the H2 cells in A. The abscissa shows the distance from each H2 cell to its next neighbor. The ordinate gives the cell number. The total number of cells (N), the mean distance to the nearest neighbor (M.D.) and the standard deviation (S.D.) are indicated. The histogram has been fit by a Gaussian function of the same mean value and standard deviation. (C) Drawing of the dendritic tree of an H2 horizontal cell and of the cell bodies of the H2 neighbors (taken from Fig. 2B). Most dendrites are confined to the territory defined by the seven neighbors (frame in A:  $470 \times 520 \mu\text{m}$ , in C:  $220 \times 155 \mu\text{m}$ ).

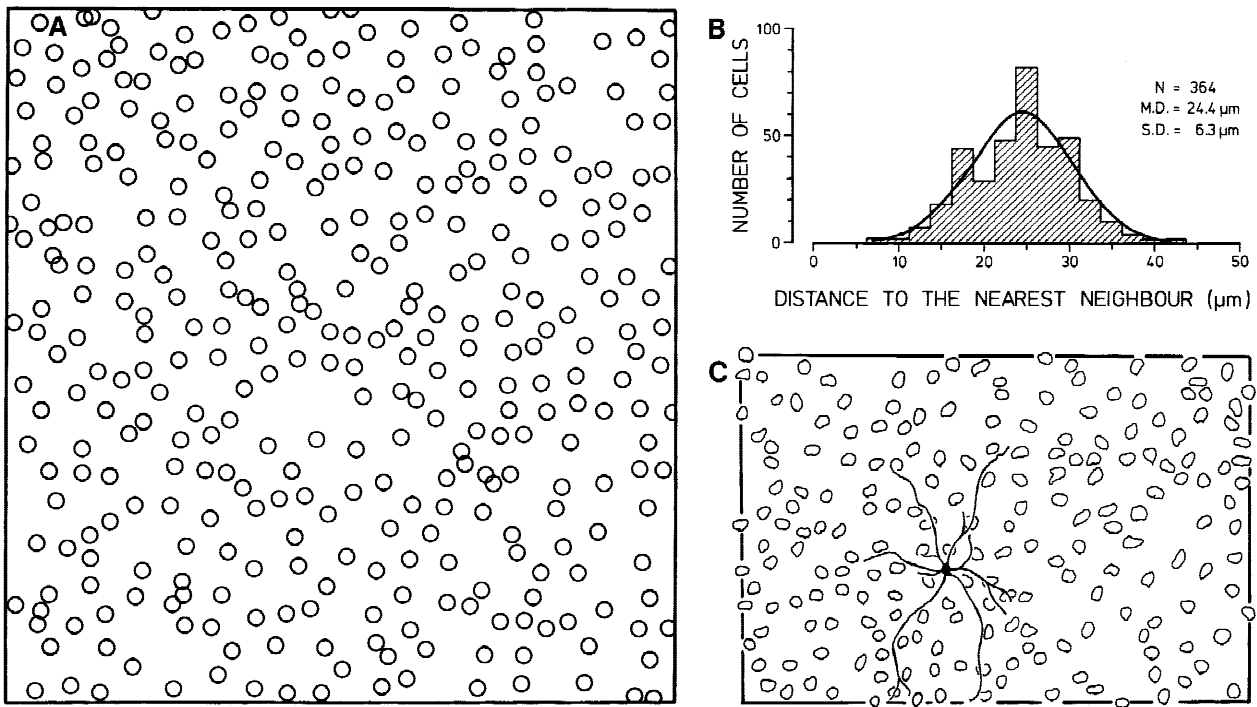


**Fig. 4.** (A) Drawing of the H1 horizontal cell mosaic taken from the Neurobiotin-injected retina shown in Fig. 1B. Circles of 15- $\mu\text{m}$  diameter represent the cell bodies. (B) Nearest-neighbor histogram and Gaussian approximation calculated from the H1 cell mosaic in A. (C) Drawing of the dendritic tree of an H1 horizontal cell and of the cell bodies of the surrounding H1 cells. The dendritic tree covers a large area and is not confined to the area defined by the immediate neighbors (frame in A: 600  $\times$  660  $\mu\text{m}$ , in C: 330  $\times$  500  $\mu\text{m}$ ).

trees of H2 cells were nicely filled with Neurobiotin, while only the somata of H1 cells appeared to be labeled. Comparable to Figs. 3 and 4, we also performed a nearest-neighbor analysis for the combined mosaic of Fig. 5 (not shown). As a first step, we considered only the mosaic of H1 cells and found a mean distance to the nearest-neighbor of 21.8  $\mu\text{m}$  (s.d. 4.2  $\mu\text{m}$ ) and a regularity index of 5.2. Next, we performed the same analysis for only the H2 cells (nearest-neighbor distance 31.7  $\mu\text{m}$ , s.d. 8  $\mu\text{m}$ , regularity index 3.9). Finally, for each cell, independent of the particular type, we measured the distance to the next neighbor (nearest-neighbor distance 16.8  $\mu\text{m}$ , s.d. 4.5  $\mu\text{m}$ , regularity index 3.73). One would expect the nearest-neighbor distance of the combined mosaic to be smaller than that of the individual mosaics. The regularity index, however, is comparable, suggesting that the H1 and H2 cells are not arrayed completely independently. It is possible, that some interaction between their mosaics during retinal development creates this overall regularity.

The cone density in the patch of Fig. 5 was 3750/mm<sup>2</sup>, the density of H1 cells was 1186/mm<sup>2</sup>, and that of H2 cells was 512/mm<sup>2</sup>. On this basis the ratio of cones to H1 cells is approximately 3, the ratio of cones to H2 cells is about 7, and the ratio of H1 cells to H2 cells is close to 2. In this peripheral patch of retina, therefore, there are twice as many H1 cells as H2 cells.

The labeling of the combined mosaics allowed differences between the two cell types at the same retinal location to become more salient. For example, H2 cell bodies were usually smaller and were often shifted to a more inner position in the inner nuclear layer (INL) as compared to H1 cells. The primary dendrites of H2 cells were more delicate than those of H1 cells and appeared to be more wavy. After having "trained" our eyes on the combined H1/H2

Neurobiotin-labeled mosaics, we were able to separate the horizontal cells in parvalbumin-immunostained retinal whole mounts (Röhrenbeck et al., 1989).

#### *Immunocytochemical staining of H1 and H2 horizontal cells with antibodies against calcium-binding proteins*

In a previous study of the monkey retina, we found that antibodies against parvalbumin and calbindin label a variety of cell types in all three nuclear layers. In the outer part of the INL, parvalbumin immunoreactivity labeled H1 and H2 horizontal cells (Röhrenbeck et al., 1989) while calbindin immunoreactivity was present in one type of horizontal cell and two types of diffuse bipolar cells (Röhrenbeck et al., 1989; Martin & Grünert, 1992; Grünert et al., 1994).

The micrograph of Fig. 6 shows a retinal whole mount that was immunostained for parvalbumin. From the information presented above, it is possible to recognize the two types of horizontal cells. H1 cells are only weakly stained and have larger cell bodies. H2 cells are more darkly stained: they have smaller cell bodies, that are often inserted further into the INL, and from which fine, wavy dendrites originate. These differences are more obvious when inspecting the cells directly on the microscope. Fig. 7A shows a drawing of the H1 and H2 cells in a larger area, including the area shown in Fig. 6. A nearest-neighbor analysis performed on the separate and combined mosaics of the two cell types (Figs. 7B–7D) gave regularity indices of 4 for the H2 cell mosaic (Fig. 7B), 5.2 for the H1 cell mosaic (Fig. 7C), and 4.7 for their combined mosaics (Fig. 7D). This is in good agreement with the results from Neurobiotin labeling.

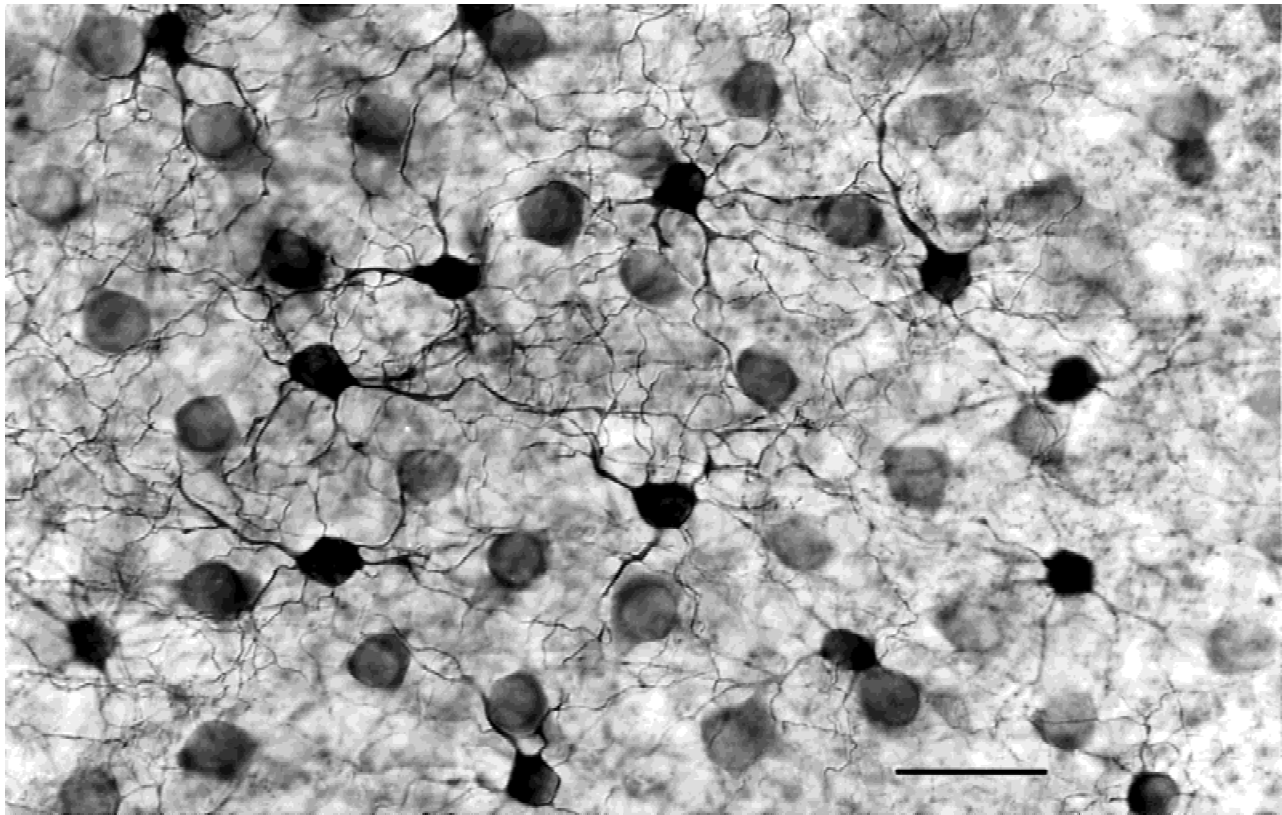


**Fig. 5.** Nomarski micrograph of tracer-coupled H1 and H2 horizontal cells following intracellular injection of Neurobiotin. H2 cells are more intensely labeled and their delicate, wavy dendrites are apparent. Only the cell bodies of H1 cells are labeled. Scale bar = 25  $\mu\text{m}$ . Eccentricity = 11.2 mm.

It is more difficult to analyze the distribution of horizontal cells and bipolar cells in the calbindin-immunostained retinal whole mounts. To gain additional and independent information, we studied retinal sections that were double labeled for parvalbumin and calbindin (Figs. 8A and 8B), and for parvalbumin and Pep 19 (Figs. 8C and 8D). Pep 19, a protein originally purified from the cerebellum, is also expressed in different cell types of the mammalian retina (Berrebi et al., 1991). Fig. 8E is a low-power micrograph of a vertical section through the central retina that was immunolabeled for parvalbumin. The horizontal cells in the outer INL, along with some amacrine cells in the inner INL and most cells of the ganglion cell layer (GCL), have been labeled. Bipolar cells do not appear to be labeled. Most of the horizontal cell somata are close to the INL/OPL border (Figs. 8A and 8E): a few, usually smaller ones, hold a more inner position. The section shown in Fig. 8A was also double labeled for calbindin (Fig. 8B). Two types of bipolar cells with axons descending into the IPL were labeled (not shown): one was the DB3 bipolar cell (Martin & Grünert, 1992; Grünert et al., 1994), the other one was a putative ON bipolar cell (DB5) with an axon terminal in the inner IPL. This cell type was more weakly stained and the axon could not always be observed (Röhrenbeck et al., 1989; Grünert et al., 1994). In contrast to our previous findings (Röhrenbeck et al., 1989), we never observed these bipolar cells to be double labeled for parvalbumin and calbindin. However, parvalbumin and calbindin were colocalized in horizontal cells (arrows in Figs. 8A and 8B). The doubled-labeled horizontal cells had smaller cell bodies, that were often inserted further into the INL, suggesting that these are H2 horizontal cells.

The parvalbumin-labeled section shown in Fig. 8C was also labeled for Pep 19 (Fig. 8D). As indicated by the arrows in Figs. 8C and 8D, the major portion of horizontal cells appears to be double labeled, while a small fraction, once again those with smaller cell bodies at a more inner position, was not double labeled. This suggests that parvalbumin labels both H1 and H2 horizontal cells, while Pep 19 immunofluorescence is present in H1 cells but not in H2 cells.

We performed a quantitative analysis on sections that were double labeled for parvalbumin and calbindin, taken from two locations: one group of sections was from midperipheral retina (eccentricity 4–5 mm) and the other group was from more central retina (eccentricity 2–3 mm). The analysis was performed on 20 double-labeled micrographs containing altogether 685 horizontal cells. From the sections we calculated the ratios of H1 and H2 cells allowing for their different cell body sizes (H1: 6.7  $\mu\text{m}$ ; H2: 5.2  $\mu\text{m}$ ) by applying the Abercrombie correction (Abercrombie, 1946). The ratio of H1 to H2 cells was 4 to 1 in the central retina and 2.8 to 1 in the region of the optic nerve head. These data, together with data from parvalbumin-labeled whole mounts (Table 2) and from Neurobiotin-injected patches (Table 1), show that there is a change in the relative proportions of H1 and H2 cells with eccentricity: in central retina the ratio of H1 to H2 cells is 4 to 1, in midperipheral retina 3 to 1, and in peripheral retina 2 to 1.

The study of the Neurobiotin-injected H2 cells and the analysis of their mosaic (Figs. 2 and 5) provided the criteria for recognition of H2 cells in calbindin-labeled horizontal sections (Fig. 9) and enabled their separation from the two types of bipolar cells. To improve the penetration of the antibodies, horizontal sections of



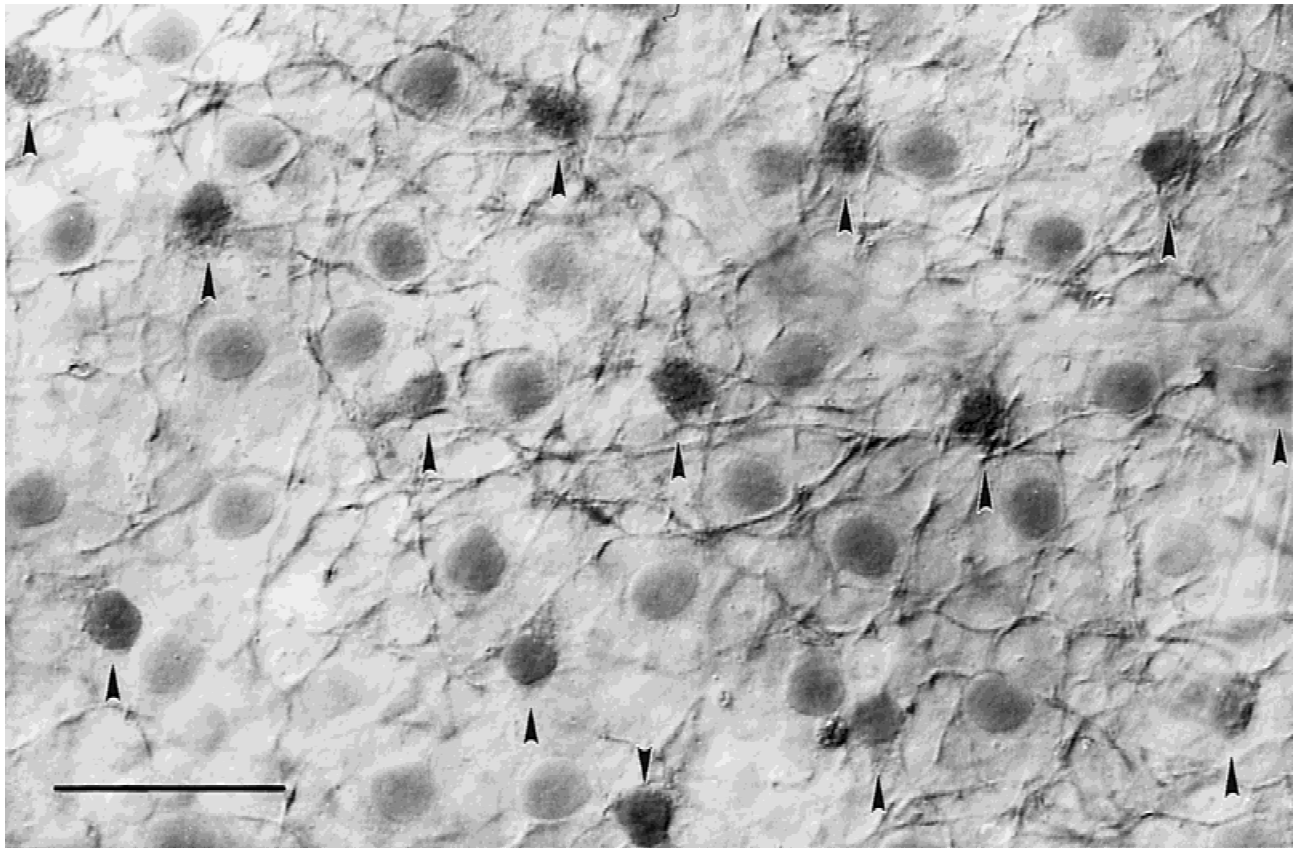


**Fig. 6.** Nomarski micrograph of a retinal whole mount that was immunostained for parvalbumin (PV). Both H1 and H2 horizontal cells are stained. H2 cell bodies (arrowheads) are smaller and more darkly labeled. H1 cells are weakly labeled and only the nucleus is apparent. Scale bar = 25  $\mu\text{m}$ . Eccentricity = 5.6 mm.

70- $\mu\text{m}$  thickness were immunostained instead of retinal whole mounts. Fig. 9 shows the calbindin labeling in such a section. It is difficult to recognize the H2 cells (see arrowheads) in the micrographs. However, by direct inspection in the microscope DB3 cells can be recognized from their descending axons and their more darkly stained cell bodies (Grünert et al., 1994). H2 cells in Fig. 9 could be separated from the ON bipolar cells because the primary dendritic branches of H2 cells were often stained and their cell bodies were larger and kept an outer position in the INL.

#### *The number of horizontal cells contacted by an individual cone pedicle*

At an eccentricity of 0.5 mm to 1 mm the cone pedicle density peaks at about 32,000 pedicles per  $\text{mm}^2$  (Wässle et al., 1989a), and the total horizontal cell density has a maximum of 23,000 per  $\text{mm}^2$  (Röhrenbeck et al., 1989). In the present study, we have found in sections that were double labeled for parvalbumin and calbindin (Fig. 8) a ratio of H1 to H2 cells close to the fovea of 4 to 1. On this basis a peak density of 4600 H2 cells per  $\text{mm}^2$  is estimated. Close to the fovea H2 cells contact about 15 cones (Boycott et al., 1987; Wässle et al., 1989a). The number of H2 cells contacted by an individual cone pedicle (divergence) can be calculated as 2.2 ( $15 \times 4600/32,000$ ). At an eccentricity of 5–6 mm in temporal retina the cone density is about 6000 per  $\text{mm}^2$  (Wässle et al., 1989b), and the H2 cell density in parvalbumin immuno-

stained retinae in the present study (Table 2) was estimated to be 1000 per  $\text{mm}^2$ . At that eccentricity H2 cells contact in Golgi-stained retinae between 16 and 22 cones (Wässle et al., 1989b). The number of horizontal cell contacted by an individual cone pedicle (divergence) would be between 2.7 and 3.7 ( $16 \times 1000/6000$ ;  $22 \times 1000/6000$ ). For the peripheral, Neurobiotin-injected patch (Fig. 3) we have estimated a divergence of 2.74. These data show that across the retina an individual cone pedicle contacts approximately 2–3 different H2 cells.

Using the same approach, we can also estimate the number of H1 cells contacted by an individual cone pedicle. Close to the fovea the peak density of H1 cells is 18,400 cells per  $\text{mm}^2$  and H1 cells there contact 6–7 cone pedicles (density: 32,000/ $\text{mm}^2$ ). On this basis the divergence from cone pedicles to H1 cells is 3.7 ( $6.5 \times 18,400/32,000$ ). In midperipheral retina (eccentricity: 5–6 mm, temporal retina), the H1 cell density has dropped to 2500 cells per  $\text{mm}^2$ , and the numbers of cones contacted has increased to about 18 at a cone density of 6000 per  $\text{mm}^2$ . From these densities the number of H1 cells an individual cone pedicle contacts would be 7.5 ( $18 \times 2500/6000$ ). For the peripheral, Neurobiotin-injected patch we have estimated a divergence of 9 (Fig. 4).

#### *H2 horizontal cells misplaced into the ganglion cell layer*

In the Neurobiotin-stained patches of H2 horizontal cells, we noticed a small proportion of stained cells, in the ganglion cell layer

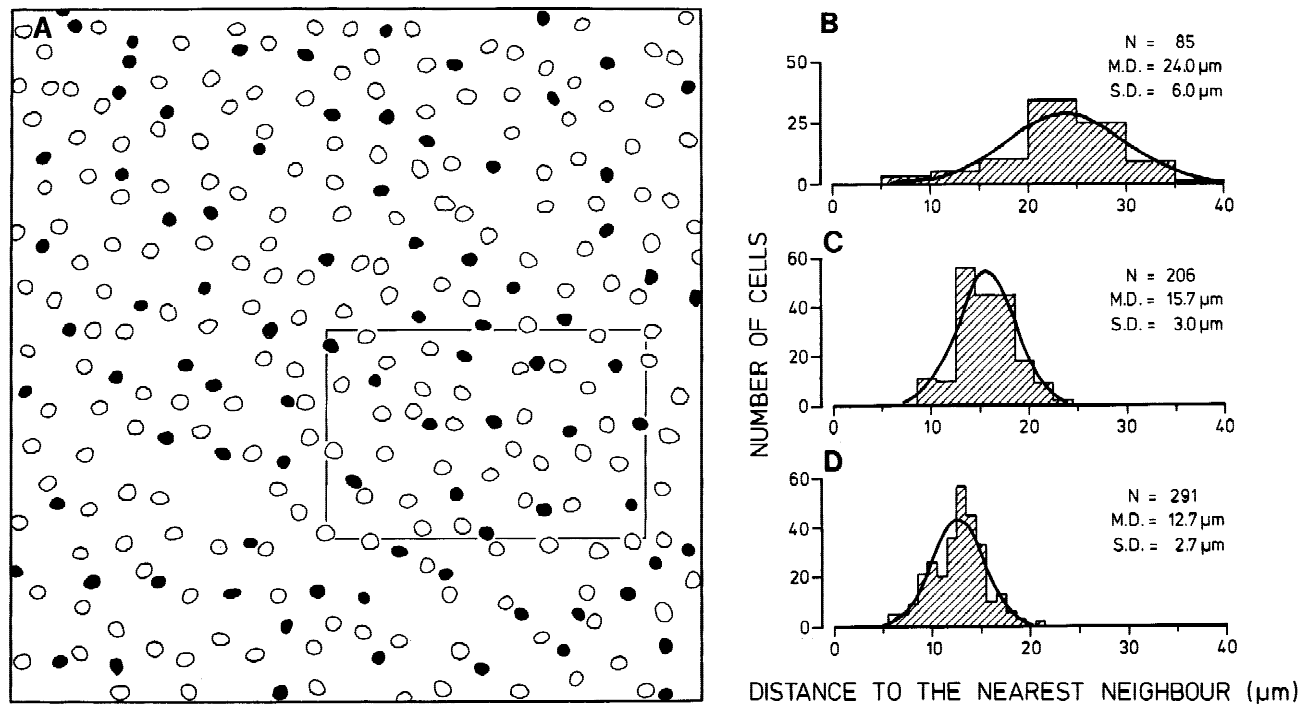


**Fig. 7.** (A) Drawing of the mosaic of H1 cells (open circles) and H2 cells (filled circles) from a parvalbumin-labeled retinal whole mount. The rectangular insert shows the same field as the micrograph in Fig. 6. (B) Nearest-neighbor histogram of the H2 cells shown in A. (C) Nearest-neighbor histogram of the H1 cells shown in A. (D) Nearest-neighbor histogram of the combined mosaic of H1 and H2 cells shown in A (frame size of A: 300  $\mu\text{m}$   $\times$  300  $\mu\text{m}$ ).

(GCL). The cells were obviously dye coupled with the H2 cells; they had comparable labeling intensities, cell body sizes, and cytoplasmic features. They had small irregular dendritic fields in the IPL and, most importantly, one or several processes that ascended through the IPL and INL and terminated in the OPL amongst the aggregates of H2 cell processes contacting cone pedicles. We suggest that the ascending processes are connected through gap junctions to the processes of regular H2 cells and that these are the sites of tracer coupling. An axon entering the optic nerve fiber layer and heading toward the blind spot was never observed on these cells. An example of a misplaced cell and the overlaying H2 horizontal cell patch is shown in the Figs. 10A and 10B. The arrow indicates the ascending "biplexiform" process of this cell. We interpret these cells as misplaced H2 horizontal cells. In the Neurobiotin-stained H2 cell patches analyzed in the present study, 762 H2 cells were encountered and 23 misplaced H2 cells were observed, suggesting that 3% of the H2 cells are misplaced. We never observed any misplaced cells among the patches of stained H1 cells. Misplaced horizontal cells in the ganglion cell layer have been observed in other mammalian retinas (Silveira et al., 1989; Peichl & Gonzales-Soriano, 1994) and appear to be errors in retinal development. This is illustrated quite convincingly by the micrographs of Fig. 11, showing A-type horizontal cells of the cat retina immunolabeled for calbindin. With the focus on the outer retina (Fig. 11A), the regular mosaic and dendritic network of the A-type horizontal cells becomes apparent. With the focal plane in the ganglion cell layer, several "typical" A-type horizontal cells that are obviously misplaced can be detected.

After observing these irregular H2 horizontal cells in the Neurobiotin-labeled patches, we also found them both in the

parvalbumin- and calbindin-immunostained whole mounts. They are much more darkly stained than the weakly labeled amacrine or ganglion cells (Figs. 10C and 10D). Their irregular dendritic branches are well stained and on nearly every cell one or several fine processes ascending into the outer plexiform layer could be observed. We wanted to find out if these cells form a regular mosaic and if their dendrites provide a homogeneous tiling of the retina. From a calbindin-immunostained retinal whole mount, we drew all these cells in a piece of retina 3.6 mm by 3.6 mm wide (Fig. 12A). Each cell is surrounded by a circle (diameter: 150  $\mu\text{m}$ ), which represents the largest dendritic field observed in this field. The distribution of these cells in Fig. 12A shows that they are irregularly arrayed and that there are large areas which are devoid of them. The six cells in the rectangle in the lower left corner of Fig. 12A are shown at higher magnification in Fig. 12B. Their dendritic trees appear quite asymmetrical and, at the positions marked by the arrows, ascending processes were observed. The total H2 cell mosaic within this field was drawn by changing the focus of the microscope into the OPL (Fig. 12C). There were 104 H2 cells in this field; the six irregular H2 cells represent 5% of the population. In the whole mounts, we systematically searched for these irregular H2 cells at different retinal locations. They were absent from the central retina. We also looked through several well-stained whole mounts of different individuals and found tremendous variability. Misplaced H2 cells accounted for approximately 5% of the cells in the ganglion cell layer of a parvalbumin-labeled retinal whole mount. The field analyzed was from midperipheral nasal retina.

These are all signs of an irregular cell type (Sandell & Masland, 1989). We have given the analysis of these irregular H2 cells so

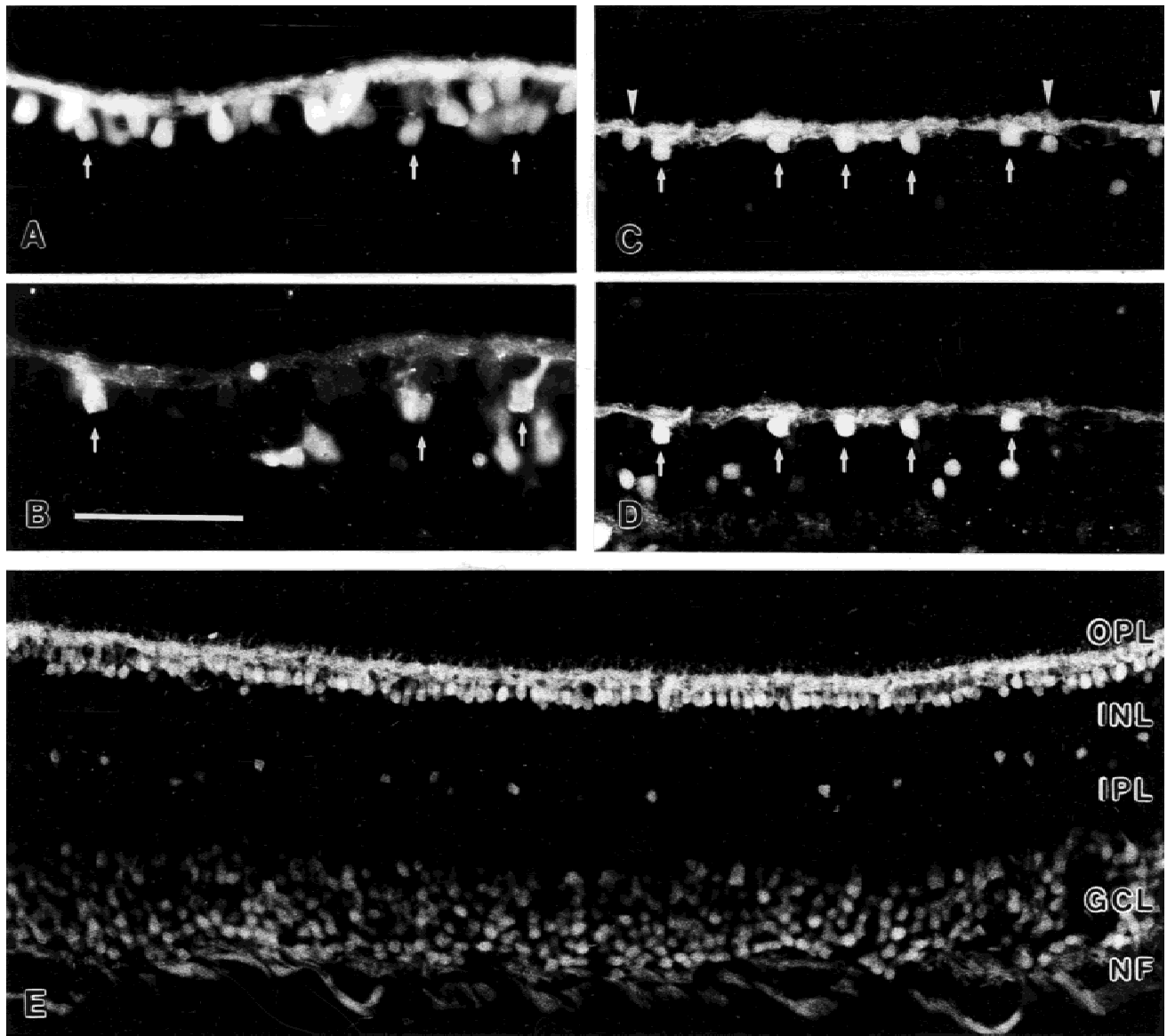


**Fig. 8.** Fluorescence micrographs of vertical sections through the outer plexiform layer of monkey retinae that were immunolabeled for horizontal cell markers. (A) Section from the foveal slope showing 21 horizontal cell perikarya immunoreactive for parvalbumin. Three labeled cell bodies (arrows) appear smaller and are shifted more towards the inner retina. (B) Same section as in A showing calbindin immunofluorescence. The arrows point to three putative H2 cells that were double labeled for parvalbumin and calbindin. The other labeled cell bodies represent bipolar cells. (C) Section from the region of the blind spot immunolabeled for parvalbumin. Eight horizontal cell bodies can be distinguished (3 arrowheads, 5 arrows). (D) Same section as in C but immunolabeled for Pep19. Comparison of C and D shows that five horizontal cells (arrows) are double labeled, while three horizontal cells (arrowheads in C) are not. The unlabeled cells are smaller, more inner, and most likely represent H2 cells. Some bipolar and amacrine cell bodies are also immunoreactive for Pep19. (E) Low-power micrograph from the central retina labeled for parvalbumin (OPL: outer plexiform layer; INL: inner nuclear layer; IPL: inner plexiform layer; GCL: ganglion cell layer; and NF: optic nerve fiber layer. Scale bar = 38  $\mu\text{m}$  in A and B; 50  $\mu\text{m}$  in C and D; and 75  $\mu\text{m}$  in E.

much emphasis here because we think they are identical to the bipelexiform ganglion cells, that were described as a new type of retinal neuron some years ago (Mariani, 1982; Zrenner et al., 1983). In addition they have been given prominence in the retinal anatomy sections of two new textbooks (Rodieck, 1998; Oyster, 1999).

We observed numerous such cells in a Golgi-stained whole mount of a macaque monkey retina (kindly provided by Dr. R. W. Rodieck). Two examples are illustrated in the micrographs of Fig. 13.

The cell in Fig. 13A has a cell body in the GCL and keeps its dendritic branches in the inner part of the IPL. The axon of an invaginating midget bipolar cell (arrow in Fig. 13A) terminates at the same level. When the focus is changed towards the OPL, two ascending processes could be seen to originate from the bipelexiform cell and terminate in the OPL (Fig. 13B). The meandering process in Fig. 13B is very reminiscent of an H2 cell axon (Kolb et al., 1980; Mariani, 1984; Gallego, 1985; Boycott et al., 1987), and clusters of terminals (arrowheads) can be observed. Figs. 13C

**Table 2.** The density of horizontal cells and cones measured from immunostained monkey retinae<sup>a</sup>

Patch (animal)	Eccentricity (mm)	H1-cell density (1/mm <sup>2</sup> )	H2-cell density (1/mm <sup>2</sup> )	Cone density (1/mm <sup>2</sup> )	H1/H2 ratio
1 (9.8.99)	2–3	6360	1586	—	4/1
2 (99.5/18.1)	3.5	4700	1600	12000	2.9/1
3 (29.7.99)	4–5	2665	947	5035	2.8/1
4 (97.3/17.3)	5.6	2278	933	5417	2.4/1
5 (96.5/18.2)	6.3	1950	1150	5400	1.8/1
6 (101.9/26.7)	7.1	1914	1133	5195	1.7/1

<sup>a</sup>Patches 1 and 3 represent sections that were double labeled for parvalbumin and calbindin. All the other patches represent measurements from retinal whole mounts immunostained for parvalbumin.

and 13D show another bplexiform cell that has the cell body and the dendritic tree in the inner retina (Fig. 13C), while an ascending process terminates in a thin axon-like process in the OPL (Fig. 13D). Two diffuse bipolar cells (Boycott & Wässle, 1991) are also stained:

the axon terminal of a putative ON bipolar cell is in focus in Fig. 13C (left arrow) that of an OFF bipolar cell is out of focus (right arrow in Fig. 13C). With the focus in the OPL the dendritic fields of both bipolar cells can be seen (arrows, Fig. 13D). Most of the bplexiform cells in the Golgi-stained whole mount showed the morphological features illustrated in Fig. 13. An axon entering the optic nerve fiber layer and heading towards the optic disk was never observed. However, in many cells an axon-like process meandering for some distance in the inner retina and then ascending to the OPL was observed. Since many H2 horizontal cells were also labeled in this whole mount, the striking similarity between their axons and those of bplexiform cells became apparent. However, we also observed dendritic processes on these cells ascending towards the OPL and terminating in little swellings (terminal aggregates). The morphology of these bplexiform cells in the Golgi-stained whole mounts strongly supports our assumption that they are irregular H2 horizontal cells.

## Discussion

In this study, we were able to directly determine the densities of peripheral H1 and H2 cells from patches of Neurobiotin-labeled

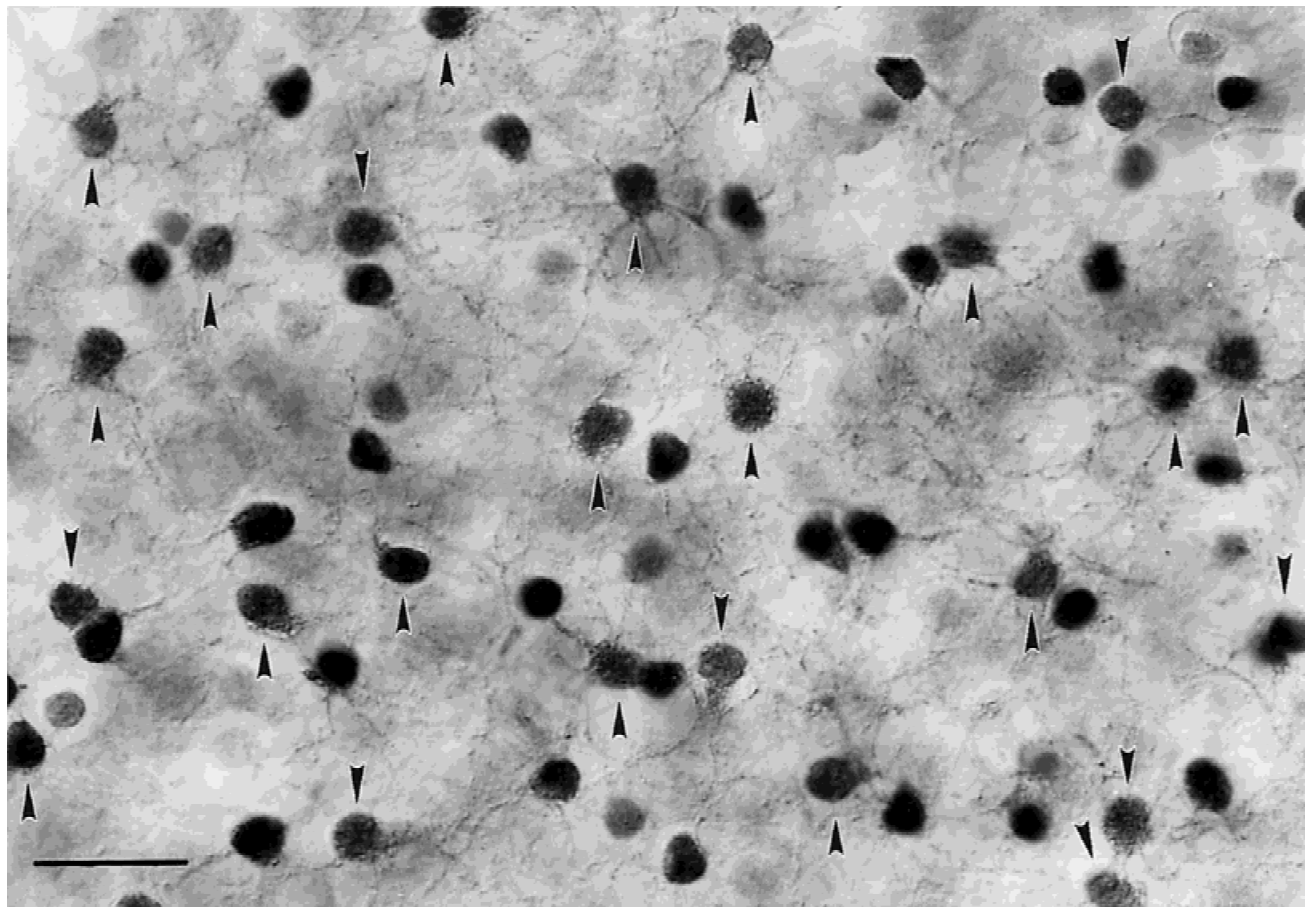


**Fig. 9.** Nomarski micrograph of retinal horizontal section that was immunostained for calbindin. The focus is on the border between the outer plexiform (OPL) and inner nuclear layers (INL). Of the 65 cell bodies in this micrograph, 25 were classified on the microscope as H2 cells (arrowheads) while 40 were classified as bipolar cells. H2 cells never had axons; they were more lightly labeled and often their primary dendritic tree could be recognized. Bipolar cells appeared more darkly labeled, they were usually smaller and in many cells an axon projecting into the inner plexiform layer could be detected. Scale bar = 25  $\mu$ m. Eccentricity, nasal retina = 13 mm.

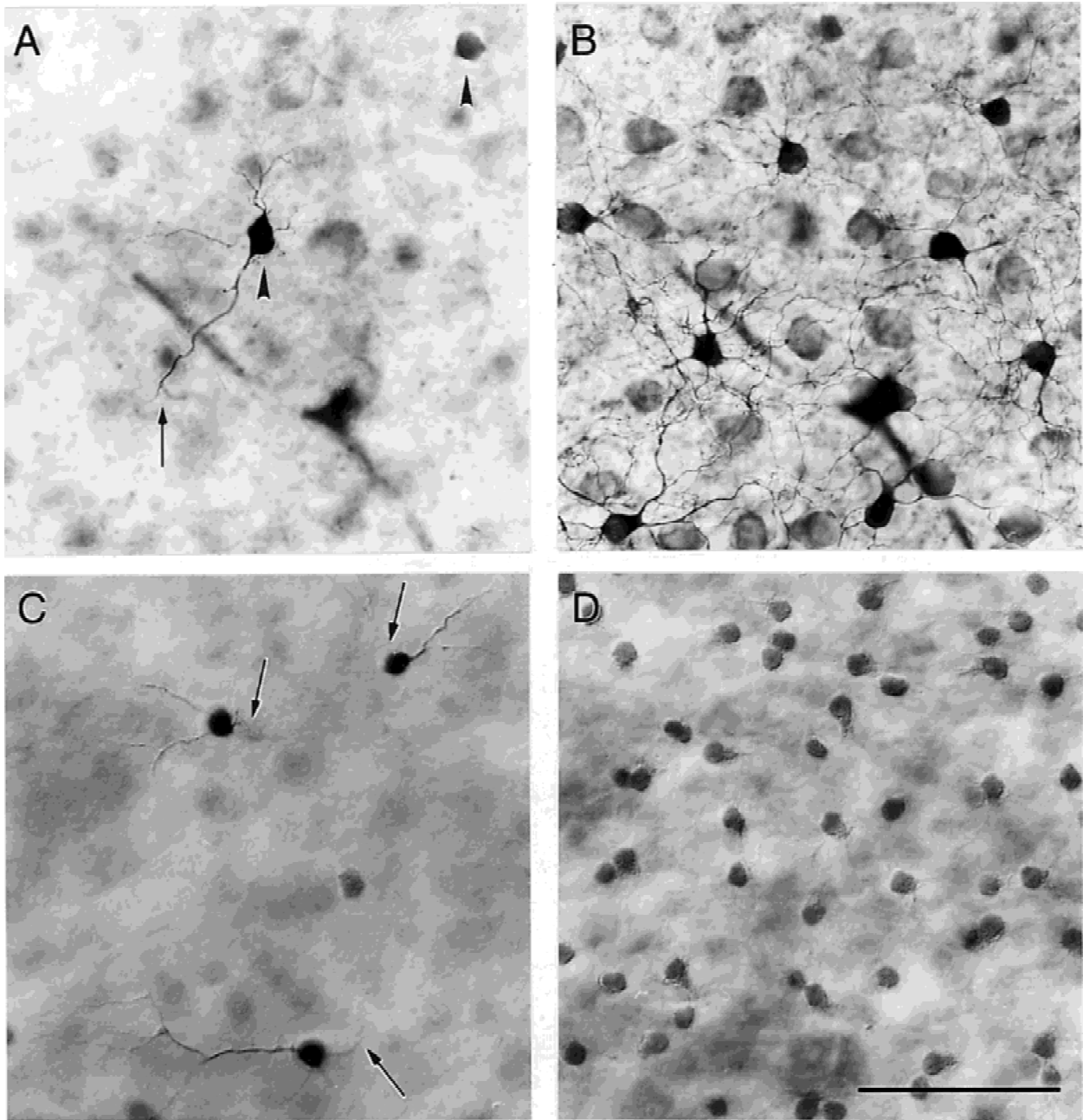


**Fig. 10.** (A) Nomarski micrograph showing the ganglion cell layer of a retina where Neurobiotin had been injected into H2 horizontal cells. Two small cell bodies (arrowheads) appear to be Neurobiotin labeled. The one in the center of the patch has a stained process (arrow) that projects into the OPL (not shown). (B) Same field of retina with the focal plane at the OPL/INL border. H2 horizontal cell bodies and dendrites are intensely labeled, and H1 cell perikarya are lightly labeled. A diagonally running blood vessel can be seen both in A and B. (C) Nomarski micrograph showing the ganglion cell layer of a calbindin-immunolabeled retinal whole mount. Three small cell bodies and irregular dendritic trees are darkly labeled. On all three cells, processes that project towards the OPL could be detected with high-power objectives (not shown). (D) Same field of retina with the focal plane at the OPL/INL border. H2 horizontal cell and bipolar cell perikarya are labeled. Scale bar = 50  $\mu\text{m}$ . Eccentricity = 11.2 mm in A and B and 11.5 mm in C and D.

retinae which revealed for the first time the mosaics of these cells (Dacey et al., 1996). Although only patches from peripheral retina were stained, these were crucial because they displayed the relationship between cone density, horizontal cell density, and the number of cones contacted by individual horizontal cells. In addition, the Neurobiotin-labeled patches showed the salient features of the horizontal cell mosaics, making it possible to separate mid-

peripheral H1 and H2 cells in parvalbumin-immunolabeled retinal whole mounts. Finally, new results from sections that were double labeled for calbindin and parvalbumin made it possible to estimate the density of horizontal cells close to the fovea. In a preceding study, only an indirect estimate of the densities of H1 and H2 cells across the retina was possible (Wässle et al., 1989b). This previous study suggested that the ratio of H1 to H2 cells is higher centrally

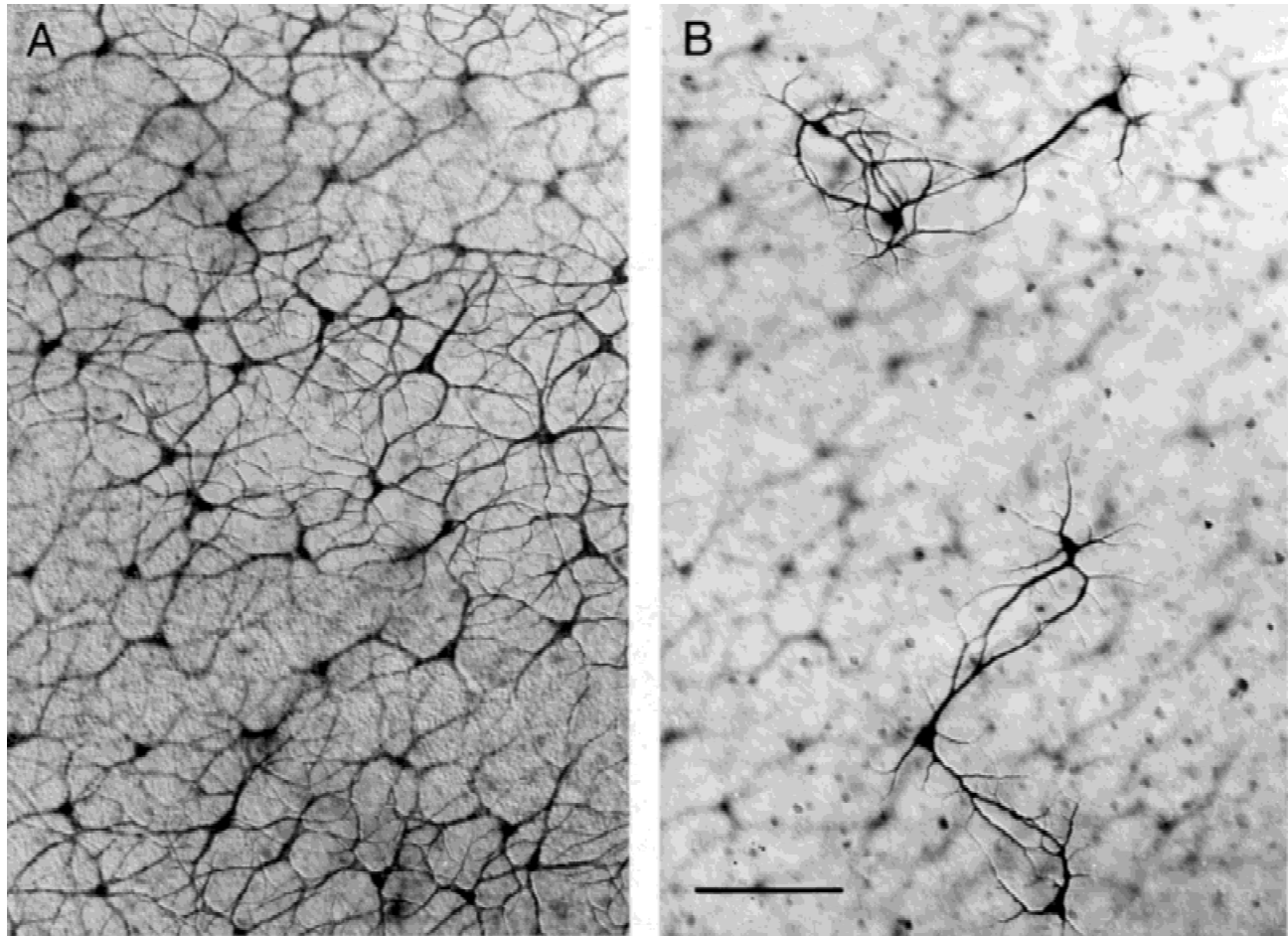


**Fig. 11.** Nomarski micrographs of whole mount of a cat retina that was immunolabeled for calbindin. (A) With the focal plane at the OPL/INL border, the dendritic network of labeled A-type horizontal cells can be seen. (B) With the focal plane in the ganglion cell layer, several misplaced A-type horizontal cells are obvious. Scale bar = 100  $\mu\text{m}$ .

but reverses peripherally, and that both H1 and H2 cells maintain constant coverage across the retina. The present study shows this not to be the case.

#### *The mosaic of H2 and H1 horizontal cells*

H1 cells outnumber H2 cells at all retinal eccentricities. The ratio of H1 and H2 cells, however, decreases from about 4 to 1 near the fovea to about 2 to 1 in the peripheral retina. Our data show that the number of H2 cells contacted by an individual cone pedicle (divergence) remains fairly constant across the retina, with each cone contacting about 2–3 H2 cells. This apparent uniformity (constancy) could be achieved by two simple rules. First, an individual H2 cell contacts all cone pedicles within its dendritic field. Second, the dendritic tree of an individual H2 cell is restricted to the area (territory) delineated by the cell bodies of its neighbors.

H2 cells contact cones both through their dendrites and their axons, and while their dendrites appear to contact all cones within their field, the axon has been thought to contact only S cones (Kolb et al., 1980), though Chan and Grünert (1998) have recently added some doubt to that picture. The above statement on constant coverage holds true only for the dendritic contacts of H2 cells.

The number of H1 cells contacted by a single cone, on the other hand, appears to increase with eccentricity, from about 3.7 H1 cells

contacted close to the fovea, to about nine in the far periphery. This increase from central towards peripheral retina is unexpected and contradicts the idea of a constant coverage of horizontal cells across the retina (Wässle et al., 1989b). However, more recent data on the number of ribbons and triads within cone pedicles are in accord with such an increase (Chun et al., 1996). The results of the Chun et al. (1996) study indicate that central cones contain about 21 ribbons while peripheral cones contain about 42. The peripheral cone pedicle thus can accommodate 84 horizontal cell terminals (two lateral elements per ribbon). If they are divided evenly among the nine H1 cells and three H2 cells, this allows for an average of seven lateral elements per horizontal cell. An individual horizontal cell can thus make multiple contacts with all its cones (Boycott & Kolb, 1973; Ahnelt & Kolb, 1994a,b; Chan et al., 1997).

#### *Immunocytochemical labeling of monkey horizontal cells with antibodies against calcium-binding proteins*

Unfortunately, no exclusive immunocytochemical marker that specifically recognizes H1 or H2 cells of the monkey retina has been found so far. Pep 19 in the present study labeled H1 cells and showed, when applied at low and moderate concentrations, no crossreactivity with H2 cells. However, Pep 19 immunofluorescence was also found in some bipolar cells. In the central retina,

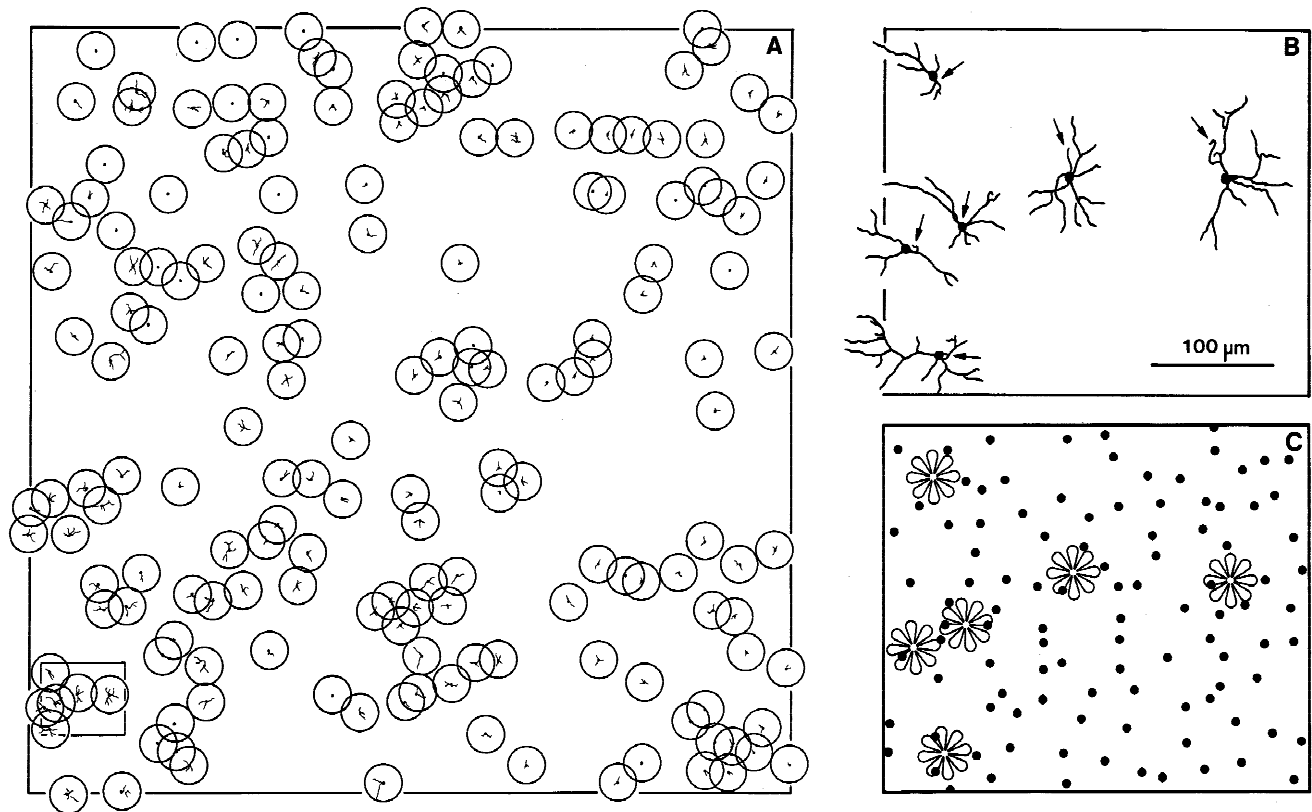


**Fig. 12.** (A) Drawings of the putative misplaced H2 horizontal cells from the peripheral monkey retina (eccentricity = 11.5 mm) immunostained for calbindin. Circles are drawn around the cell bodies which represent the maximum dendritic-field diameter (150  $\mu\text{m}$ ) observed in that field. The insert in the lower left corner is shown at higher magnification in B and C. (B) Six misplaced H2 cells and their dendritic fields. The three cells in the lower left are the same cells shown in the micrograph of Fig. 10C. (C) Same field as in B, but with the focal plane at the OPL/INL border. The dots represent the cell bodies of H2 horizontal cells, and the flower symbols represent those of misplaced cells.

the bipolar cell bodies are located more towards the center of the INL. However, in peripheral retina their cell bodies also occur in between the horizontal cell bodies in the outer INL, making cell identification more difficult.

As previously described (Röhrenbeck et al., 1989; Martin & Grünert, 1992; Grünert et al., 1994), calbindin immunoreactivity is found in horizontal cells, DB3 bipolar cells, and an ON-diffuse bipolar cell. In a previous study (Grünert et al., 1994), it was possible to separate DB3 cells and estimate their relative densities because of their well-stained axons and axon terminals. In the present study, we used horizontal sections instead of whole-mounted retinæ, hence the penetration of the calbindin antibodies was improved resulting in better staining of dendritic trees. This, together with a better understanding of H2 cell morphology as revealed in the Neurobiotin-stained patches, made it possible to recognize H2 cells in the calbindin-stained horizontal sections. On this basis, we estimate that 40% of the calbindin-immunoreactive neurons in the outer INL are H2 cells and 60% of them appear to be bipolar cells. These relative proportions were found to hold for the central and peripheral retina. Haley et al. (1995) have reported a decrease of calbindin expression towards central primate retina. In agreement with these data, we find that cones close to the fovea lose their calbindin immunoreactivity (unpublished observation). However, H2 cells and bipolar cells continue to be immunoreactive for calbindin right to the foveal pit.

In a previous study, parvalbumin immunoreactivity was found in both H1 and H2 cells (Röhrenbeck et al., 1989). However, cones and bipolar cells were also weakly labeled with the antibodies against parvalbumin (Fig. 5 of Röhrenbeck et al., 1989). During the last 10 years several antisera against parvalbumin that labeled neither cones nor bipolar cells in sections of primate retinae became commercially available (Fig. 8E). We therefore conclude that the antiserum against parvalbumin used previously exhibited a small crossreactivity with calbindin. In the present study of parvalbumin-labeled retinal whole mounts, we were able to separate H1 and H2 horizontal cells and thus study their mosaics at different eccentricities (Table 2).

#### *Irregular or misplaced H2 horizontal cells*

In the Neurobiotin-stained patches of H2 horizontal cells, we noticed a small proportion of H2 cells that were obviously displaced into the ganglion cell layer. Most importantly all these cells had, in addition to a small dendritic tree in the IPL, one or more processes that ascended into the OPL. We assume that these "interplexiform processes" are engaged in gap junctions with the regular H2 cells in the OPL and that these gap junctions are the sites of tracer coupling.

The most parsimonious explanation of these cells is to classify them as irregular H2 cells, misplaced into the ganglion cell layer.

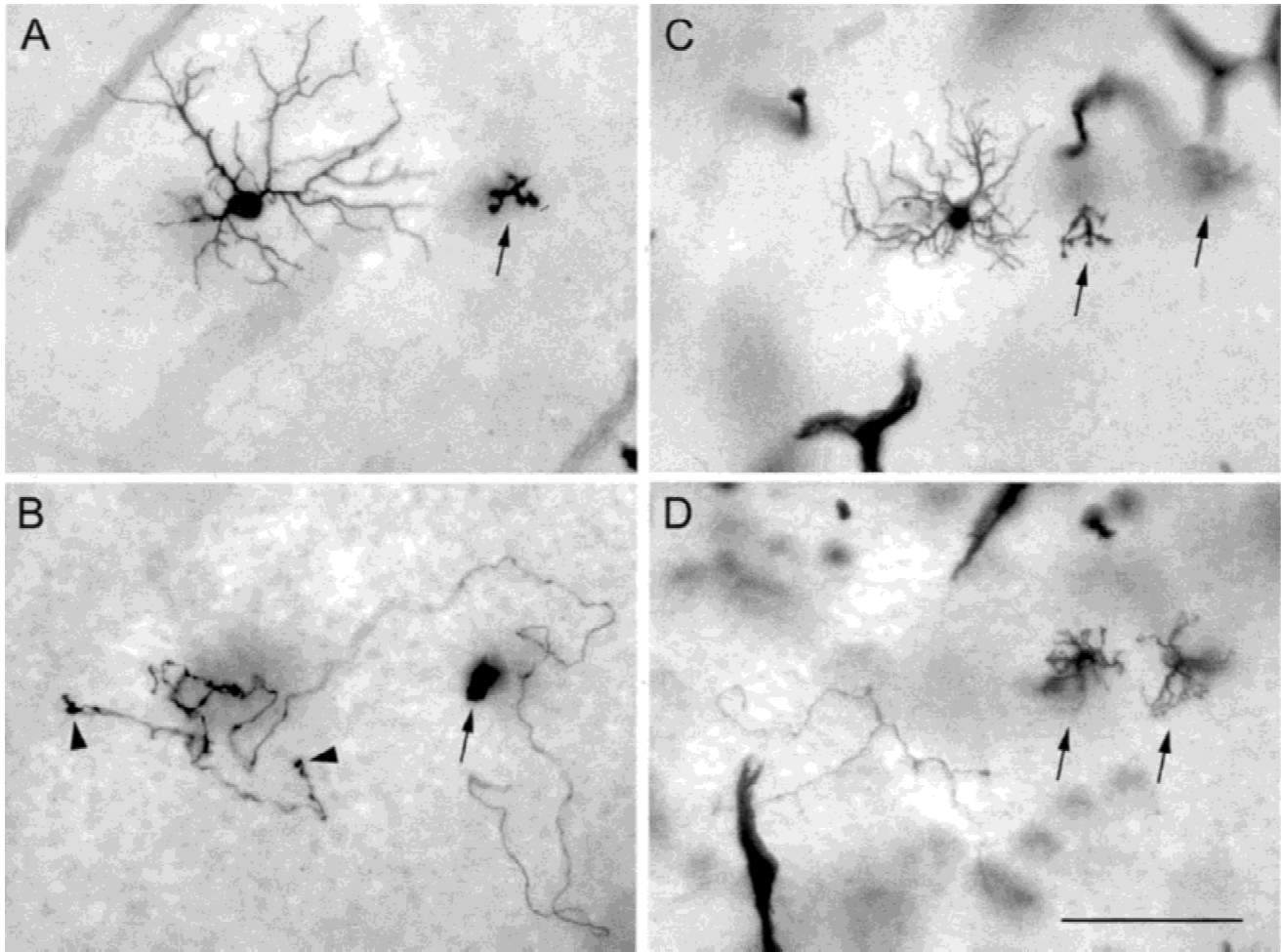


**Fig. 13.** Micrographs from a Golgi-Colonnier stained whole mount of a macaque monkey retina, kindly provided by Dr. R.W. Rodieck (Rodieck, 1989). A and B show the same cell. The focus in A was in the inner IPL. The arrow indicates the axon terminal of an ON-midget bipolar cell. The focus in B was in the OPL. The arrowheads indicate terminal aggregates that represent possible contacts with photoreceptors. The arrow points to the dendritic top of the midget bipolar cell. C and D show two similar focal planes of another cell. The thick black profiles are stained blood vessels. The arrows indicate two diffuse bipolar cells. Scale bar = 50  $\mu\text{m}$ .

Such obviously misplaced horizontal cells have been reported in different mammalian species before (Silveira et al., 1989; Peichl & Gonzales-Soriano, 1994) and have also been demonstrated here for the cat retina (Fig. 11). These irregular H2 cells together with their biplexiform processes were also strongly labeled in both parvalbumin- and calbindin-labeled retinal whole mounts and it was possible to study their mosaic across the retina. They are preferentially found in peripheral retina, and have an irregular mosaic, exhibiting many holes, or patches of higher coverage. An axon heading towards the optic nerve head was never observed in these cells. However, some of them had asymmetric, long dendrites.

Mariani (1982) described ganglion cells of the primate retina that contacted photoreceptors through ascending processes and named them biplexiform cells. Later they were referred to as “biplexiform ganglion cells” (Zrenner et al., 1983; Rodieck, 1998). Biplexiform ganglion cells have a small cell body ( $\sim 9 \mu\text{m}$  diameter), and small dendritic trees ( $\sim 100 \mu\text{m}$  diameter), with delicate, wavy dendrites. One or several processes ascend from the IPL through the INL towards the OPL where they appear to contact rod spherules as the central elements of the triads. The cells receive

unusual synapses on their dendrites in the IPL: rod bipolar cells make conventional synapses, not ribbon synapses as usual, with biplexiform ganglion cells. The evidence for an axon on these cells is sparse. Mariani (1982) observed 19 such cells in Golgi-stained retinae. Only seven of them had an axon: four were impregnated up to only  $10 \mu\text{m}$  and three were impregnated up to only  $300 \mu\text{m}$ . Zrenner et al. (1983) recorded intracellularly from three “biplexiform ganglion cells,” and filled the cells with horseradish peroxidase (HRP). The cells exhibited graded depolarizations at both light ON and light OFF. One cell with an axon was illustrated: the axon coursed  $300 \mu\text{m}$  through the IPL, before descending abruptly to the optic nerve fiber layer, and heading towards the optic nerve head.

We propose that “biplexiform ganglion cells” and misplaced H2 cells are the same cell type. As shown in Fig. 13, their descriptions have many features in common, such as the small cell body in the ganglion cell layer, the irregular small dendritic tree, some asymmetric long processes, that might be mistaken for axons, and most importantly, the interplexiform processes ascending from the inner plexiform layer towards the outer plexiform layer. The graded



potentials recorded in biphixiform ganglion cells (Zrenner et al., 1983) are the electrical signature of horizontal cells (Dacheux & Raviola, 1990; Dacey et al., 1996) and *not* of ganglion cells which fire action potentials (De Monasterio & Gouras, 1975). Horizontal cells are hyperpolarized at light ON and depolarized at light OFF (Dacheux & Raviola, 1990; Dacey et al., 1996), while interplexiform cells are depolarized both at light ON and at light OFF (Zrenner et al., 1983). This possibly reflects their input from rod bipolar cells in the IPL and from photoreceptors in the OPL (Mariani, 1982).

However, there are some discrepancies between the descriptions of the two cell types. One is the presence of an axon in biphixiform ganglion cells. The evidence, however, is based on a single somewhat atypical axon of an HRP-injected cell (Zrenner et al., 1983). Evidence for axons from Golgi staining, as described above, is only limited (Mariani, 1982). We have observed many (50) such cells in a Golgi-stained whole mount and did not observe an axon heading towards the optic disk in any cell. Another discrepancy is the synaptic connections of interplexiform ganglion cells with rods in the OPL described by Mariani (1982). Regular H2 cells contact cone pedicles as lateral elements within the triads; only a few contacts with rod spherules have been described (Kolb et al., 1980). The synaptic contacts of biphixiform ganglion cells with rod bipolar cells in the IPL is also unusual (Mariani, 1982). Rod bipolar cells of the primate retina usually make ribbon synapses at which both postsynaptic partners are amacrine cells (Grünert & Martin, 1991). To resolve these discrepancies, it will be important to look at the Golgi-stained biphixiform cells described in the present study at the electron-microscopic level, where it will be possible to determine the synaptic contacts these cells make in both the OPL and the IPL.

## References

- ABERCROMBIE, M. (1946). Estimation of nuclear population from microtome sections. *Anatomical Record* **94**, 239–247.
- AHNELT, P. & KOLB, H. (1994a). Horizontal cells and cone photoreceptors in primate retina: A Golgi light-microscopic study of spectral connectivity. *Journal of Comparative Neurology* **343**, 387–405.
- AHNELT, P. & KOLB, H. (1994b). Horizontal cells and cone photoreceptors in human retina: A Golgi electron-microscopic study of spectral connectivity. *Journal of Comparative Neurology* **343**, 406–427.
- BERREBI, A.S., OBERDICK, J., SANGAMESWARAN, L., CHRISTAKOS, S., MORGAN, J.I. & MUGNAINI, E. (1991). Cerebellar Purkinje cell markers are expressed in retinal bipolar neurons. *Journal of Comparative Neurology* **308**, 630–649.
- BOYCOTT, B.B. (1988). Horizontal cells of mammalian retinae. *Neuroscience Research* **8**, 97–111.
- BOYCOTT, B.B. & KOLB, H. (1973). The horizontal cells of the rhesus monkey retina. *Journal of Comparative Neurology* **148**, 115–140.
- BOYCOTT, B.B., HOPKINS, J.M. & SPERLING, H.G. (1987). Cone connections of the horizontal cells of the rhesus monkey's retina. *Proceedings of the Royal Society B (London)* **229**, 345–379.
- BOYCOTT, B.B. & WÄSSLE, H. (1991). Morphological classification of bipolar cells of the primate retina. *European Journal of Neuroscience* **3**, 1069–1088.
- CHAN, T.L. & GRÜNERT, U. (1998). Horizontal cell connections with short wavelength-sensitive cones in the retina: A comparison between New World and Old World primates. *Journal of Comparative Neurology* **393**, 196–209.
- CHAN, T.L., GOODCHILD, A.K. & MARTIN, P.R. (1997). The morphology and distribution of horizontal cells in the retina of a New World monkey, the marmoset *Callithrix jacchus*: A comparison with macaque monkey. *Visual Neuroscience* **14**, 125–140.
- CHUN, M.-H., GRÜNERT, U., MARTIN, P.R. & WÄSSLE, H. (1996). The synaptic complex of cones in the fovea and in the periphery of the macaque monkey retina. *Vision Research* **36**, 3383–3395.
- DACEY, D.M. & BRACE, S. (1992). A coupled network for parasol but not midgenet ganglion cells in the primate retina. *Visual Neuroscience* **9**, 279–290.
- DACEY, D.M., LEE, B.B., STAFFORD, D.K., POKORNY, J. & SMITH, V.C. (1996). Horizontal cells of the primate retina: Cone specificity without spectral opponency. *Science* **271**, 656–659.
- DACEY, D.M. (1999). Primate retina: cell types, circuits and color opponency. *Progress in Retinal and Eye Research* **18**, 737–763.
- DACHEUX, R.F. & RAVIOLA, E. (1990). Physiology of HI horizontal cells in the primate retina. *Proceedings of the Royal Society B (London)* **239**, 213–230.
- DE MONASTERIO, F. M. & GOURAS, P. (1975). Functional properties of ganglion cells of the rhesus monkey retina. *Journal of Physiology* **251**, 167–195.
- FREED, M.A., SMITH, R.G. & STERLING, P. (1987). Rod bipolar array in the cat retina: Pattern of input from rods and GABA-accumulating amacrine cells. *Journal of Comparative Neurology* **266**, 445–455.
- GALLEGO, A. (1985). Advances in horizontal cell terminology since Cajal. In *Neurocircuitry of the Retina*, ed. GALLEGO, A. & GOURAS, P., pp. 122–140. New York: Elsevier Science Publishing.
- GOODCHILD, A.K., CHAN, T.L. & GRÜNERT, U. (1996). Horizontal cell connections with short-wavelength-sensitive cones in macaque monkey retina. *Visual Neuroscience* **13**, 833–845.
- GRÜNERT, U. & MARTIN, P.R. (1991). Rod bipolar cells in the macaque monkey retina: Immunoreactivity and connectivity. *Journal of Neuroscience* **11**, 2742–2758.
- GRÜNERT, U., MARTIN, P.R. & WÄSSLE, H. (1994). Immunocytochemical analysis of bipolar cells in the macaque monkey retina. *Journal of Comparative Neurology* **348**, 607–627.
- HALEY, T.L., POCHE, R., BAIZER, L., BURTON, M.D., CRABB, J.W., PARMENTIER, M. & POLANS, A.S. (1995). Calbindin D-28K immunoreactivity of human cone cells varies with retinal position. *Visual Neuroscience* **12**, 301–307.
- KOLB, H. (1970). Organization of the outer plexiform layer of the primate retina: Electron microscopy of Golgi-impregnated cells. *Philosophical Transactions of the Royal Society B (London)* **258**, 261–283.
- KOLB, H. (1991). Anatomical pathways for color vision in the human retina. *Visual Neuroscience* **7**, 61–74.
- KOLB, H., FERNANDEZ, E., SCHOUTEN, J., AHNELT, P., LINBERG, K.A. & FISHER, S.K. (1994). Are there three types of horizontal cell in the human retina? *Journal of Comparative Neurology* **343**, 370–386.
- KOLB, H., LINBERG, K.A. & FISHER, S.K. (1992). Neurons of the human retina: A Golgi study. *Journal of Comparative Neurology* **318**, 147–187.
- KOLB, H., MARIANI, A. & GALLEGO, A. (1980). A second type of horizontal cell in the monkey retina. *Journal of Comparative Neurology* **189**, 31–44.
- MARIANI, A.P. (1982). Biphixiform cells: Ganglion cells of the primate retina that contact photoreceptors. *Science* **216**, 1134–1136.
- MARIANI, A.P. (1984). The neuronal organization of the outer plexiform layer of the primate retina. *International Review of Cytology* **86**, 285–320.
- MARTIN, P.R. & GRÜNERT, U. (1992). Spatial density and immunoreactivity of bipolar cells in the macaque monkey retina. *Journal of Comparative Neurology* **323**, 269–287.
- MILLS, S.L. & MASSEY, S.C. (1994). Distribution and coverage of A- and B-type horizontal cells stained with Neurobiotin in the rabbit retina. *Visual Neuroscience* **11**, 549–560.
- OYSTER, C.W. (1999). *The Human Eye*. Sunderland, Massachusetts: Sinauer Assoc.
- PEICHL, L. & GONZÁLEZ-SORIANO, J. (1994). Morphological types of horizontal cell in rodent retinae: A comparison of rat, mouse, gerbil, and guinea pig. *Visual Neuroscience* **11**, 501–507.
- PINOL, M.R., KÄGI, U., HEIZMANN, C.W., VOGEL, B., SÉQUIER, J.-M., HAAS, W. & HUNZIKER, W. (1990). Poly- and monoclonal antibodies against recombinant rat brain calbindin D-28K were produced to map its selective distribution in the central nervous system. *Journal of Neurochemistry* **54**, 1827–1833.
- RODIECK, R.W. (1989). Starburst amacrine cells of the primate retina. *Journal of Comparative Neurology* **285**, 18–37.
- RODIECK, R.W. (1998). *The First Steps in Seeing*. Sunderland, Massachusetts: Sinauer Assoc.
- RÖHRENBECK, J., WÄSSLE, H. & BOYCOTT, B.B. (1989). Horizontal cells in the monkey retina: Immunocytochemical staining with antibodies against calcium binding proteins. *European Journal of Neuroscience* **1**, 407–420.

- SANDELL, J.H. & MASLAND, R.H. (1989). Shape and distribution of an unusual retinal neuron. *Journal of Comparative Neurology* **280**, 489–497.
- SILVEIRA, L.C.L., YAMADA, E.S. & PÍCANÇO-DINIZ, C.W. (1989). Displaced horizontal cells and biphaxiform horizontal cells in the mammalian retina. *Visual Neuroscience* **3**, 483–488.
- STERNBERGER, L.A. & STERNBERGER, N.H. (1986). The unlabeled antibody method: Comparison of peroxidase-antiperoxidase with avidin-biotin complex by a new method of quantification. *Journal of Histochemical Cytochemistry* **34**, 599–605.
- STICHEL, C.C., KÄGI, U. & HEIZMANN, C.W. (1986). Parvalbumin in cat brain: Isolation, characterization, and localization. *Journal of Neurochemistry* **47**, 46–53.
- VANEY, D.I. (1991). Many diverse types of retinal neurons show tracer coupling when injected with biocytin or Neurobiotin. *Neuroscience Letters* **125**, 187–190.
- VANEY, D.I. (1992). Photochromic intensification of diaminobenzidine reaction product in the presence of tetrazolium salts: Applications for intracellular labelling and immunohistochemistry. *Journal of Neuroscience Methods* **44**, 217–223.
- VANEY, D.I. (1993). The coupling pattern of axon-bearing horizontal cells in the mammalian retina. *Proceedings of the Royal Society B (London)* **252**, 93–101.
- VANEY, D.I. (1994). Patterns of neuronal coupling in the retina. *Progress in Retinal Eye Research* **13**, 301–355.
- WÄSSLE, H., LEVICK, W.R. & CLELAND, B.G. (1975). The distribution of the alpha type of ganglion cells in the cat's retina. *Journal of Comparative Neurology* **159**, 419–438.
- WÄSSLE, H. & RIEMANN, H.J. (1978). The mosaic of nerve cells in the mammalian retina. *Proceedings of the Royal Society B (London)* **200**, 441–461.
- WÄSSLE, H., GRÜNERT, U., RÖHRENBECK, J. & BOYCOTT, B.B. (1989a). Cortical magnification factor and the ganglion cell density of the primate retina. *Nature* **341**, 643–646.
- WÄSSLE, H., BOYCOTT, B.B. & RÖHRENBECK, J. (1989b). Horizontal cells in the monkey retina: Cone connections and dendritic network. *European Journal of Neuroscience* **1**, 421–435.
- ZIAI, R., PAN, Y.-C.E., HULMES, J.D., SANGAMESWARAN, L. & MORGAN, J.I. (1986). Isolation, sequence, and developmental profile of a brain-specific polypeptide, PEP-19. *Proceedings of the National Academy of Sciences of the U.S.A.* **83**, 8420–8423.
- ZRENNER, E., NELSON, R. & MARIANI, A. (1983). Intracellular recordings from a biphaxiform ganglion cell in macaque retina, stained with horseradish peroxidase. *Brain Research* **262**, 181–185.